# Rendering Plasma Phenomena: Applications and Challenges

G.V.G. Baranoski[1] and J.G. Rokne[2]

[1] Natural Phenomena Simulation Group, School of Computer Science, University of Waterloo, Canada
[2] Department of Computer Science, The University of Calgary, Canada

**Abstract**

*Plasmas are ubiquitous in the Universe. An understanding of plasma phenomena is therefore of importance for almost every area of astrophysics, from stellar atmospheres to star clusters. Plasmas also occur in daily life both in industrial processes and in consumer products. Recent groundbreaking data is making this the golden age of plasma science. Although direct observations and analysis of data provide important physical evidence for plasma phenomena, they do not necessarily explain the phenomena. Hence, recent discoveries in this area might not only arise out of observations, but also from visual simulations of the phenomena supported by advanced rendering technologies. This report describes the state of art of such simulations, and examines practical issues often overlooked in the literature. Their educational and public outreach applications are also discussed. Although the emphasis is on the predictive rendering of plasma processes, the simulation guidelines and trade-offs addressed in this report can be extended to the general simulation of natural phenomena. The report closes with a discussion of further avenues of research involving the simulation of plasma phenomena.*

Categories and Subject Descriptors (according to ACM CCS): I.3.7 [Computer Graphics]: Three-Dimensional Graphics and Realism I.6.8 [Simulation and Modeling]: Types of Simulation J.2 [Computer Applications]: Physical Sciences and Engineering

**Keywords:** plasma, rendering, simulation, natural phenomena

## 1. Introduction

The simulation of natural phenomena is an evolving area of research where significant progress has been made. However, until recently, the natural processes involving plasmas remained relatively unexplored their impressive manifestations and scientific importance. Following the growing academic and industrial interest in plasma science and its applications [Nat95, Nat03, Jos06], the visual simulation of these processes is now attracting the attention of a larger segment of the computer graphics community.

In order to understand plasma phenomena, a combination of extensive data analysis, theory, modeling, laboratory experiments and *in situ* (space born) observation is required [NC01, Nat03]. Recent efforts in this area resulted in the gathering of valuable data for the study of plasma processes [SGK*02, GN02]. Furthermore, advances are being made with the use of computer simulations supported by effective rendering algorithms [CJP02, LDY02].

While computer graphics researchers have the expertise in the development of rendering tools, scientists and engineers from a myriad of fields, from physics to chemistry, are taking advantage of their practical use. As a contribution to these synergistic research efforts, this report examines not only recent computer graphics works on the rendering of plasma phenomena, but also visual simulations done by researchers in other scientific fields working in the forefront of plasma science.

This report begins by defining plasma and providing relevant plasma concepts and terminology. A brief description of the principles involved in the interactions of plasma particles with matter in other states, especially gas, is also presented. These interactions may result in photon (light) emissions

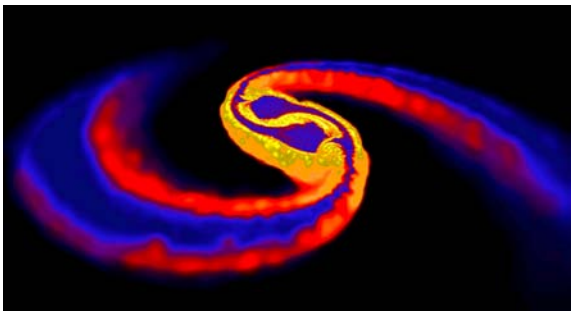

**Figure 1:** *Frame from an animation sequence simulating the collision of two neutron stars. Courtesy of D.J. Price and S. Rosswog.*

**Figure 2:** *Frame from an animation sequence simulating the dynamics of an auroral band.*

which are responsible by the exquisite colors observed in phenomena such as aurorae and space nebulae (Section 2.3). Although the focus of this report is on computer graphics issues, an outline of the numerical simulation methods used to model these processes is provided to support the examination of different approaches used to render plasma phenomena.

In the context of this report, these rendering approaches are classified as either illustrative or realistic. The former aim at the generation of images that depict specific characteristics of a given phenomena (Figure 1), whereas the latter aim at the generation of images that provide a plausible visual representation of a given phenomena (Figure 2). Both types have been used to render phenomena such as solar events (magnetic loops, solar convection and coronal mass ejections), lightning discharges, aurorae (also known as Northern or Southern lights) and space nebulae. Relevant simulation issues related to the rendering of these phenomena are examined in this report.

Since plasma phenomena are often associated with characteristic spectral displays, reproducing their visual appearance is one way of evaluating plasma theories and models. However, there are guidelines and constraints, such as the availability of supporting data, the reliability of the evaluation approach to be used, and the trade-off between accuracy and computational cost, that need to be taken into account to achieve this goal. These methodological issues are discussed along with practical rendering aspects such as illumination mapping solutions for high dynamic range scenes and spectral color reproduction. The discussion is illustrated by examples involving recent work on the rendering of plasma phenomena. It is worth noting that the relevance of these issues is not limited to the visual simulation of plasma events. In fact, researchers working on physically-based rendering have been raising similar questions for many years [GAL*97, LRP97, DCWP02, BB03].

Along with recent technological advances in terms of measurement and experimental devices, simulation and rendering algorithms can provide a pivotal contribution to the solution of open problems involving plasma phenomena. Accordingly, the report closes with an outlook on these avenues of research.

## 2. What is Plasma?

In this section, we provide an overview of plasma properties, and define terms used throughout this report. The reader interested in more information about plasma physics is referred to comprehensive texts on this topic [Bit04, Che84, Das04, GR95, GB05]. We also discuss plasma-matter interactions responsible for visual manifestations of plasma phenomena, and we briefly outline the main numerical simulation approaches and models used in the study of plasma dynamics. For a detailed description of these approaches and models, we recommend the texts by Hockney and Eastwood [HE88], Birdsall and Langdon [BL91], and Eastwood [Eas93].

### 2.1. General Properties and Definition

Plasmas usually occur at high temperatures as a result of a phase transition process that may be perceived as a logical step in a sequence of phase transitions from the other states of matter. For this reason, they are designated as “the forth state of the matter” [Bit04, Che84, GR95]. For instance, when heat is applied to a solid, the thermal motion of the atoms can break the crystal lattice structure, and a liquid may be formed. Similarly, when liquid is heated sufficiently, atoms may vaporize off the surface faster than they recondense, and a gas may be formed. Analogously, when enough heat is applied to a gas, its atoms may collide with each other and knock some of their orbital electrons out in a process known as ionization [FLS64a], and a plasma is formed. This plasma formation process also explains the usual defi-

nition of plasma as an ionized gas consisting of an approximate equal number of positively and negatively charged particles [GB05]. However, any ionized gas cannot be called a plasma since there is always some small degree of ionization in any gas [Che84], and in the remainder of this section, we therefore describe the characteristics and quantitative criteria that an ionized gas must satisfy to be called a plasma.

It is worth noting that the ionization process responsible for plasma formation can also be triggered by other mechanisms. Considering that an ordinary gas may have a small number of charged particles (*e.g.*, due to the ionizing action of cosmic rays [Ich86]), the application of a strong electrical field (an electric discharge) to these charged particles accelerate them to high energies, and when these particles collide with other atoms or molecules they ionize them. This acceleration may be also caused by exposing an ordinary gas to energetic photons [GB05]. For example, ultraviolet rays from the sun create free electrons and ions in the upper layer of the Earth's atmosphere forming the ionosphere, a plasma medium of central importance in radiowave communications [FLS64b].

The amount of ionization to be expect in a gas in thermal equilibrium is given by the Saha equation [Bit04, Che84]:

$$\frac{n_i}{n_n} \approx 2.4 \times 10^{21} \frac{T^{\frac{3}{2}}}{n_1} e^{\frac{-U_i}{KT}}, \tag{1}$$

where $n_i$ and $n_e$ represent the density (number per $m^3$) of ionized and neutral atoms respectively, $T$ corresponds to the gas temperature (given in *Kelvin*), $K$ corresponds to the Boltzmann's constant, and $U_i$ represents the ionization energy (given in $eV$) of the gas, *i.e.*, the energy required to remove the outermost electron from an atom. As the temperature is raised, the degree of ionization remains relatively low until $U_i$ is only a few times $KT$. At this point, the ratio $\frac{n_i}{n_e}$ rises abruptly, and the gas is considered to be in plasma state.

Besides high temperatures, which are responsible for the occurrence of plasma in astronomical bodies (*e.g.*, stellar interiors), another important factor may contribute to the existence of plasma in Nature, namely the density of the electrons. Once an atom is ionized, it remains charged until it meets an electron. It then may recombine with the electron to become neutral again. The recombination rate depends on the density of electrons, which one can assume to be equal to $n_i$. Hence, a relative low density of electrons (*e.g.*, in interstellar or intergalactic medium) can determine a low recombination rate, which in turn favors the occurrence of plasma [Che84].

The interplay between temperature and density also affects how the transition from ordinary particles to plasma occurs. The same way that the distinction between liquid and vapor blurs when the the liquid is heated at high pressures and becomes more violent at low pressures, the transitions observed with respect to plasmas are seamless for low densities and more dramatic for higher densities. Incidentally, the critical point of temperature and density where nuclear matter should boil in collisions and condense as the plasma cools, a process known as first-order phase transition, is an open problem in nuclear physics [Cho06].

In plasma, as charged particles move around, they can generate local concentrations of positive and negative charges, which give rise to electrical fields. This motion of the charged particles also generates currents, and hence magnetic fields. These fields in turn affect the motion of other charged particles far away. The net result is the motions of the charged particles being affected not only by local conditions, but also by the state of plasma in distant regions. This collective behavior is a fundamental characteristic of plasma. Hence, it can be more appropriately defined as a *quasineutral* gas of charged and neutral particles which exhibits *collective behavior* [Che84].

The plasma quasineutrality is related to its ability to shield out electric potentials that are applied to it. For example, when a negative test charge is placed in an homogeneous plasma, the electrons are immediately repelled and the ions are attracted, and the resulting displacement of electrons and ions produces a polarization charge that shields the plasma from the test charge [GB05]. The characteristic length over which this shielding occurs is called the Debye length [DH23], and it corresponds to the radius of the cloud of ions ("Debye sphere") around the test charge. It can be expressed by [GB05]:

$$\lambda_D = 69\sqrt{\frac{T}{n}}, \tag{2}$$

where $n$ represent plasma density, which for a quasineutral plasma can be approximated by $n \approx n_e \approx n_i$ [Che84]. When the dimensions $L$ of a plasma system are much large than $\lambda_D$, local concentrations of charge or external potentials introduced in the system are shield out in a distance short compared to $L$, leaving the rest of the system free of large potentials or fields, *i.e.*, quasineutral. Hence, the first criterion that an ionized gas has to fulfill to be designated plasma is related to its density, *i.e.*, it needs to be dense enough so that $\lambda_D << L$ [Che84]. In addition, for the Debye shielding to be statistically acceptable, it is necessary that there are enough particles in the "Debye sphere". The number $N_D$ of particles in the "Debye sphere", which also affects the plasma "collective behavior", gives the second criterion that a plasma must satisfy, namely $N_D >>> 1$ [Che84].

The third criterion is related to the collision patterns. The weakly ionized gas in a jet exhaust does not qualify as a plasma because the charged particles collide so frequently with neutral atoms that their motion is controlled by ordinary hydrodynamic forces rather then by electromagnetic forces [Che84]. When the density of the electrons in a region of undisturbed plasma system in equilibrium state increases, *e.g.*, due to some internal motion of the particles, they will repel each other and tend to return to their original

positions. As they move toward their original positions, they acquire kinetic energy. As there is little damping for electron motion, instead of coming to rest in their equilibrium configuration, the electrons overshoot the position. As a result, the electron density oscillates back and forth around its equilibrium value [FLS64b, Kil06]. If $\omega$ is the frequency of typical plasma oscillations, and $\tau$ is the mean time between collisions with neutral atoms, it is also required that $\omega\tau > 1$ for the gas to behave like a plasma [Che84].

Plasma oscillations also occur in metals [FLS64b], which contain relatively mobile, free charged particles. These particles can be regarded as a solid state plasma [Ich86], known as quantum plasma due to quantum-mechanical interference effects between neighboring electrons caused by their high density. Certain liquids, such as solutions of sodium in ammonia [Che84] or in water [FLS64b], have been found to behave like plasma as well. It is also worth mentioning ultracold plasmas (ion temperatures near 1 Kelvin) formed from laser-cooled atoms by the ionizing action of an intense laser pulse [Kil06]. These plasmas act like a liquid or a solid rather than a gaseous plasma since the interactions between the particles can dominate the particles' random thermal motions. We remark, however, that, unless otherwise stated, the term plasma used in this report refers to the standard, gaseous plasma, which is the focus of this work.

Tonks and Langmuir, who pionered the study of ionized gases in the 1920s, gave this state of the matter the name plasma after the Greek word $\pi\lambda\alpha\sigma\mu\alpha$ which means "moldable substance" [Bit04, GR95]. However, due to its collective behavior, a plasma oftens presents a large variety of possible motions that seem to suggest that it has a mind of its own as appropriately stated by Chen [Che84].

### 2.2. Natural and Man Made Plasmas

Most of the matter in the known universe exists as a plasma [Bit04]. For instance, the Sun, our nearest star, is composed of superheated gases that exist in plasma state. Nearly everything that happens in and on this thermonuclear reactor affects our planet. This is especially true for large scale plasma events such as solar flares and coronal mass ejections (CME) [Bur00]. During these events, plasma particles are emitted from the Sun primarily from highly magnetized areas in the solar photosphere known as sunspots, which have a lower temperature than the solar corona. As the sun rotates these particles are thrown out in spiraling streams, forming the "solar wind" (Figure 3), which hits the Earth's magnetosphere (the region that contains the Earth's magnetic field [Bit04]) after few days. These surges of plasma particles can cause communication blackouts, overload power lines (causing massive electrical blackouts), disable satellites, destroy delicate instruments on spacecrafts orbiting Earth, and possibly, injury or even kill a space walking astronaut [PM99, Ode00, Sup04].

Not surprisingly, many companies and governmental agencies are investing many resources in the investigation of these phenomena [Ode00]. In fact, the largest coordinate study of the Sun, known as the International Heliophysical Year (IHY), will be launched in 2007. In the same year the largest-ever fleet of space missions for studying solar-terrestrial interactions will be put at scientists disposal. This will include National Aeronautics and Space Administration (NASA) Solar Terrestrial Relations Observatory (STEREO) which consists of two craft that are going to take stereoscopic images of the Sun to track the three-dimensional structure of CMEs [Cla06], which are often associated with coronal loops. These solar phenomena (Figure 4), that can be detected at invisible (X-ray and ultraviolet), and visible light wavelengths, consist in archs extending upward from the photosphere for tens or hundreds of thousands of kilometers. Although the physical processes that cause these phenomena are not completely understood yet, recent observations from SOHO (Solar and Heliospheric Observatory), a joint European Space Agency (ESA) and NASA mission to investigate the dynamics of the Sun, and from NASA TRACE (Transition Region and Coronal Explorer) spacecraft suggested that the loops are jets of hot plasma flowing along in the regions between the strong coronal magnetic fields.

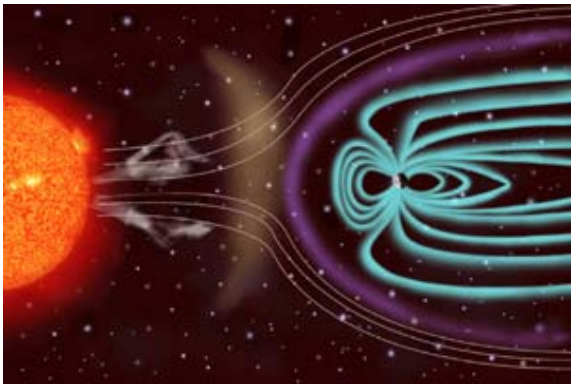

**Figure 3:** *Artist's conception of the interaction of solar wind with the Earth's magnetosphere. Courtesy of NASA/CXC/SAO).*

The magnetic storms triggered by solar flares and CME events [Bry99] are also responsible for the auroral displays that occur in the Earth and also in the other magnetized planets of the solar system [Tay01]. These displays are considered by the scientists as a visual laboratory for the investigation of plasma phenomena and "footprints" of events and energetic process occurring in the Earth's atmosphere [Aka94, BE94, Bre97, Eat80, RB67]. In fact, the impressive visual characteristics of auroral displays have fascinated writers, philosophers, poets and scientists over the centuries. The famous scientist Anders Jonas Angström, who discovered hydrogen in the solar atmosphere, was also the first person to examine the emission spectra of the aurorae [Ang69].

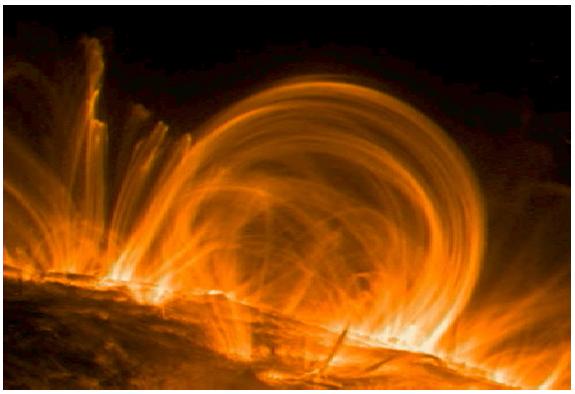

**Figure 4:** *Image illustrating actual ultraviolet observations (color coded) of coronal loops. Courtesy of NASA/GSFC/TRACE.*

**Figure 5:** *Photograph of a cloud-to-ground lightning. Courtesy of J. Myers.*

Another plasma phenomenon encountered in the Earth's atmosphere is lightning (Figure 5). Although atmospheric lightning can be classified into four different groups, namely cloud-to-ground, cloud-to-cloud, cloud-to-air and inter-cloud lightning [BOM06], the underlying physical process is the same, *i.e.*, the current present in a lightning discharge ionize and heat the atmospheric gas to a high temperature. Due to the high recombination rate, however, the resulting plasma exists only for a fraction of a second. The main process responsible for the cloud-to-ground lightning discharges commonly observed during storms and often recorded in photographs develops as follows. Starting from the cloud, electrons (charges) are accelerated towards the ground, a process known as "step leader". During their descent, the air changes into a plasma incrementally, *i.e.*, it becomes a conductor along the path, or plasma channel, through which the lightning channel will develop. The moment the leader touches the ground, the electrons at the bottom of the leader escape, leaving positive charge behind that attracts more negative charge from higher up in the leader, which in turn run out. This process continues upwards like that until all the negative charge in a part of the cloud is released along the column (lightning channel) in a fast and energetic way, causing the lightning stroke that we see, called return stroke [FLS64b]. This strokes that leaps from ground to the cloud produces the brightest light observed during an atmospheric lightning discharge.

Besides its pervasive occurrence in Nature, plasmas can also be formed through man made devices aimed at scientific and engineering applications. For example, it can be used to develop ion propulsion based engines for interplanetary missions [Bit04, Che84]. Since a plasma is a collection of mobile charged particles, it can be also perceived as an electrically conductive fluid. Thus, when an external electromagnetic field is applied to a plasma, an electric current is induced in it changing the motion of the plasma particles. This coupling of plasma motion with electromagnetic fields, which is studied in the magneto-hydrodynamics (MHD) field [Bit04, Ich86], provides the basis for the design of such engines.

Another important practical application is related to the development of energy reactors based on controlled thermonuclear fusion. In order to make fusion reactions possible, it is necessary to create a plasma in which the thermal energies are in the range of tens of $keV$. This is a complex process which is difficult to be achieved in a controlled setting. In fact, the search for a nearly limitless energy source from controlled thermonuclear fusion has been responsible for the rapid growth of plasma physics [Che84, GR95], and for the allocation of expressive amounts of financial and technical resources to the study of the problem of heating and confining such a plasma using magnetic fields (through devices known as tokamaks). As examples of recent investments in this area, we can cite the International Thermonuclear Experimental Reactor (ITER) project ($11 billion dollars) and the Chinese Experimental Advanced Superconducting Tokamak (EAST) project ($37 million dollars) [Nor06].

For decades scientists have been using particle accelerators to understand how the seemingly disparate forces in our universe are all connected. These machines use microwave cavities to propel particle beams to nearly the speed of light. This approach is reaching its technological and economical limits, however [Jos06]. A new plasma-based approach, in which electrons or positrons gain energy by surfing on a wave in plasma, might dramatically reduce the size and cost of future particle accelerators. The process works as follows.

A pulse from an intense laser or particle beam creates a disturbance in the plasma by pushing the lighter electrons away from the heavier ions. The disturbance creates a wave that travels through plasma at nearly the speed of light. A powerful electric field points from the positive to the negative region, and will accelerate any charged particle that come under its influence [Jos06]. In order to prevent that the particles become out of phase, *i.e.*, outrun the wave, several approaches can be applied. For example, by introducing a perpendicular magnetic field the particles are deflected across the wave, and they can be accelerated to high energy as they ride across the wave fronts like a surfer cutting across the face of an ocean wave, a process know as surfatron [KD83]. Although plasma-base accelerators have been only demonstrated in small scale laboratory experiments, scientists and engineers already envision tabletop accelerators for a wide range of lower-energy applications, including materials science, structural biology, nuclear medicine and food sterilization [Jos06].

### 2.3. Interactions with Light and Matter

Most of the phenomena that we can observe in Nature involve the interaction of light (photons) and matter (electrons). These interactions are described by the theory of quantum electrodynamics (QED) [Fey88]. The only phenomena not covered by this theory are those involving gravitation and nuclear forces. According to QED theory, all phenomena involving these interactions arise from three basic actions: a photon goes from place to place, an electron goes from place to place, and an electron emits or absorbs a photon. Although plasma particles are not visible by the naked eye, their interactions with atoms (or molecules) of other materials may trigger the absorption or emission of photons by orbital electrons of these atoms which in turn may result in visible manifestations of plasma phenomena. Although the main focus of this report is on these manifestations, it is important to note that invisible radiation emitted by plasmas has several scientific applications, specially in astrophysics, since they can be use to infer plasma properties [Bit04]. In this section, we provide a brief description of the main processes of light emission, thermal and luminescent, responsible for plasma phenomena manifestations. This description is illustrated by the examination of selected plasma phenomena from a spectral point of view.

As described by the QED theory, an atom in the ground state can absorb a photon and go into the excited state, and an atom in the excited state can emit a photon and go to the ground state. Thermal emissions occur when a material radiates excess heat energy in the form of light. For these materials, called thermal radiators, the amount of light emitted is primarily dependent on the ratio of the average number of atoms in the excited state ($N_g$) to the average number of atoms in the ground state ($N_g$), which relates to the material's temperature through the following expression [FLS64c]:

$$\frac{N_e}{N_g} = e^{\frac{-h}{\lambda K T}}, \tag{3}$$

where $h$ corresponds to the Planck's constant and $\lambda$ represents the wavelength of the emitted photons.

A thermal radiator of uniform temperature whose radiant exitance in all parts of the spectrum is maximum obtainable from any thermal radiator at the same temperature is called a blackbody. Although no material reaches the theoretical maximum of a blackbody, it is sometimes convenient to describe the emissive properties of a material by specifying, on a wavelength basis, the fraction of light it generates with respect to a blackbody. For example, solar radiation arrives at the Earth's atmosphere with a spectral energy distribution similar to a blackbody radiator of 5,800 Kelvin [SM81]. Blackbody radiation emitted from plasmas in thermodynamic equilibrium is of significance only for astrophysical plasmas due to the large size needed for a plasma to radiate as a blackbody [Bit04]. Accretion disks (plasma flows) around neutron stars (celestial bodies consisting of extremely dense remains of a massive star that has collapsed [OC96]) and black holes are examples of such astrophysical plasmas. When a black hole is formed in a binary star system, it can pull gas from the companion star, which will spiral toward the black hole forming an accretion disk. As the gas spirals, it is compressed and heated to millions of Kelvins and emits X-rays. Such X-ray sources have been detected (*e.g.*, through measurements made by the NASA Chandra X-ray Orbiting Observatory [GMNC01]), and used to identify black hole candidates [OC96]. The gravity of a neutron star can also cause its accretion disk to emit X-rays.

Just as a blackbody radiator can be used as a simple model for a star radiation profile, it can also be used to provide a rough first approximation for an optically thick accretion disk. According to this approximation, the disk will emit blackbody radiation with a continuous spectrum corresponding to the local disk temperature at that distance [OC96]. It is worth noting that despite their formation similarities, however, accretions disk around black holes and neutron stars emit radiation in different patterns. In addition, although in both cases a strong gravitational redshift (an increase in the wavelength of radiation in a gravitational field predicted by the general theory of relativity [Sho03]) caused by these extreme dense astrophysical objects make the disks to appear "dimmer" and "redder", when the disk material strikes the solid surface of the neutron star, it glows brightly (Figure 6).

Luminescent emissions are due to energy arriving from elsewhere, which is stored in the material and emitted (after a short period of time) as photons. The incident energy, primarily due to factors other than heat, also causes the excitation of electrons of the material. These electrons in the outer and incomplete inner shells move to a higher energy state within the atom. When an electron returns to the ground state a photon is emitted. The wavelength of the emitted photon

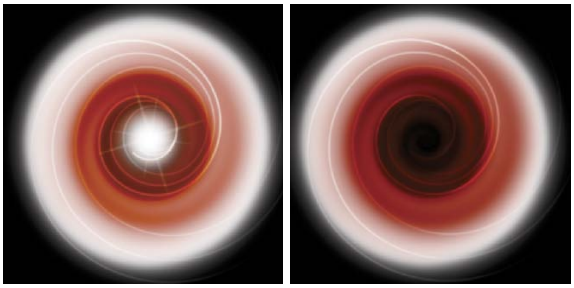

**Figure 6:** *Artist's conception of accretion disks around a neutron star (left) and a black hole (right). Courtesy of NASA/CXC/M. Weiss.*

will depend on the atomic structure of the material and the magnitude of the incoming energy. Excitation of the atoms may also occur due to the impact of high energy plasma particles, which is responsible for the impressive light emissions found in plasma phenomena such as the aurorae and nebulae as briefly described in the remainder of this section.

During interactions of solar wind with the Earth's magnetosphere (Figure 3), due to mechanisms yet unknown, highly energetic plasma particles (electrons) are accelerated towards the regions around the planet's magnetic poles and interact with atmospheric atoms. The atoms are then excited, and after a period of time they may emit a photon (in much the same way as in neon based signs and flat-panel displays). Statistically, several collisions must occur before a photon is emitted. The wavelength of this photon, a *spectral emission line*, depends primarily on the type of atmospheric constituent hit by the electron and the stability of the atom's excited state. In practice the wavelength will correlate with height. Atomic oxygen and molecular and atomic nitrogen are the principal constituents of the upper atmosphere available for and involved in the production of auroral emissions at these altitudes.

Besides the spectral emission lines generated by collisions between electrons and atoms, the auroral spectrum is also composed of *spectral emission bands* generated by collisions between electrons and molecules. The most common and the brightest visible feature of the aurorae, the atomic oxygen "green line" at 557.7$nm$, is dominant in the lower parts of auroral displays, around 100$km$. It is mainly due to this emission line that most aurorae appear yellow-green. Because the peak of human light sensitivity is about 555.0$nm$, these aurorae are particularly bright-looking. The red in the upper parts is caused mainly by another commonly observed line, the atomic oxygen "red line" at 630.0$nm$. The bluish color, seen sometimes on the lower border of auroral displays, comes mainly from the ionized nitrogen "blue band" at 427.8$nm$. The spectral variety of auroral displays is further contributed to by weaker light emissions at other wavelengths across the visible spectrum. The mixtures in various ratios of all of these components may result in a wide variety of colors.

**Figure 7:** *Photograph of an auroral drapery showing structured green emissions on the bottom and red emissions spread over the upper board. Courtesy of J. Curtis.*

Even though green and red, which are the strongest lines in the auroral spectrum, both originate from excited atomic oxygen, they behave quite differently. The transition state that produces the atomic oxygen green line only exists for up to 0.7$s$, and the excited atom cannot move far before its photon is emitted. As a result the green line is often visible in structured forms. The transition state that produces the atomic oxygen red line can exist for 110$s$, and the atom can travel a longer distance from the point at which it was excited. As a result, the red emissions are spread over a wider area. The ionized nitrogen blue band has a spatial distribution similar to the green line, since the transition state that gives rise to this band can exist for less than 0.001$s$ [BE94]. The longer the life of an excited atom, the greater the chance it has of colliding with other atmospheric particles and losing its capacity to emit light, a process known as *quenching* [Jon74]. This explains why the red oxygen line is weaker than the green line at lower altitudes (higher atmosphere density) within an auroral display, and why some auroral features are red at high altitude and green lower down (Figure 7).

The term "nebula" was originally used by astronomers to refer to any "fuzzy' patch in the sky that could be easily distinguished by a telescope, but was not sharp like stars or planets. Although the etymological root of "nebula" means "cloud", the word "nebula" is sometimes used to refer to galaxies, various types of star clusters and various kinds of interstellar dust/gas clouds. In the context of this report, the word "nebulae" is reserved for space gas and dust clouds and not for groups of stars, and the following discussion will be focused on emission and planetary nebulae [Mal89, Mal94].

**Figure 8:** *Photograph showing the emission nebula Eta Carina. Courtesy of D. Malin.*

**Figure 9:** *Photograph showing the planetary nebula Helix. Courtesy of D. Malin.*

In the same way that auroral emissions are considered “fingerprints” of the Earth’s atmosphere by geophysicists, astrophysicists deduce the chemical content of nebulae by examing their spectra.

Emission nebulae are plasma clouds composed of hydrogen and free electrons. The hydrogen atoms of the interstellar medium are ionized by the ultraviolet radiation from a nearby star or stars. Only very hot stars, typically young stars, have enough radiation in the ultraviolet region at wavelengths necessary to ionize the hydrogen. This explains why emission nebulae are usually the sites of recent and ongoing star formation. The excess energy beyond that needed to ionize the hydrogen goes to kinetic energy of the ejected electrons. Eventually, by collision, this energy is shared by other particles in the gas. As the ions fall back into lower energy states, in most cases after recombination of ions with electrons, they emit light (photons) at discrete wavelengths or spectral lines (in much the same way as the auroral emissions). The most prominent of these in the visible spectrum is the red line of hydrogen, giving most emission nebulae a characteristic red glow (Figure 8). There are also "forbidden lines" (ones not normally seen in Earth-bound laboratories) in the spectra from nebulae. Certain low probability, or “forbidden”, transitions from metastable states (without light emissions [FLS64a]) leading to radiation emission are also found in the aurorae [Jon74]. The most prominent are green lines from doubly ionized oxygen, giving some nebulae a green shading. Interspersed within the glowing gas of nebulae are lanes of dark dust which can give nebulae their characteristic appearance.

Planetary nebulae are glowing and expanding shells of gas and plasma formed around certain types of stars (white dwarfs) at the end of their lives. They received the name “planetary” in the nineteenth century because they look like giant gaseous planets when viewed through a small telescope [OC96]. This type of nebula owes its appearance to the ultraviolet light emitted by the hot, condensed central star. This ultraviolet radiation ionizes the expanding gas, and the resulting plasma is similar to that found in emission nebulae, but with more ions in higher energy levels. Therefore, the spectral emission lines from these higher states, such as the green forbidden lines of doubly ionized oxygen, are stronger in these nebulae (Figure 9). In fact, the bluish-green coloration of many planetary nebulae is due to oxygen and neon forbidden lines, and the reddish coloration comes from ionized hydrogen and nitrogen [OC96].

### 2.4. Numerical Simulation Approaches and Models

Numerical simulation approaches of plasma dynamics can be broadly divided in three types: Eulerian, Lagrangian and combinations of these [Hoc66]. The Eulerian approach assumes that plasma behaves like a fluid, *i.e.*, it obeys macroscopic differential kinetic equations for average quantities. The Lagrangian approach follows the motion of a large number of plasma particles as they move in time under their mutual electromagnetic interactions. Although this approach acts on the microscopic particle level, it allows the particle ensemble to “make its own mind” about the macroscopic and collective behavior. In a hybrid Eulerian-Lagrangian approach usually the time independent field quantities are computed using an Eulerian scheme, while the time dependent particles attributes (*e.g.*, velocity and position) are computed using a Lagrangian scheme.

At a first glance, the similarities between neutral fluids and plasma, such as the presence of shear flows (differential motions within different parts of a given material), might suggest that the computational fluid dynamics formulation would be sufficient to model the behavior of both media. However, in order to perform predictive simulations of the dynamics of plasma phenomena, one must account for their distinctive features. For example, turbulence dynamics in plasmas involve electromagnetic fields and a much larger number of relevant variables than for neutral fluids [YIIY01]. Furthermore, while the effects of global boundary conditions, such as wall boundaries, often play an important role in the growth of neutral fluid disturbances [DR81, Hin75, Yos98], plasma turbulence is greatly affected by spatial inhomogeneities and plasma configurations. These inhomogeneities are coupled together to drive or suppress turbulent fluctuations, which often have a very long correlation length along the magnetic field line and are quasi-two-dimensional [YIIY01].

Much of the recent progress in the field of plasma physics was only made possible by advances in computational methods [GPZ*04, Tan02]. Generally, an analytical, closed-form solution for the equations involved in plasma dynamics simulations is difficult to obtain [BWRB05]. One can only obtain a unique solution by imposing various restrictions [VK95], and they are normally solved using numerical methods such as finite difference (FD) [Taf00], finite volume (FV) [And01], finite element (FE) [SF90] and smoothed particle hydrodynamics (SPH) [Mon05] methods. Combinations of these methods are often used in the design of simulation models, and algorithms derived using one method may be identical to those derived using another [Eas93].

The key strategy in computational plasma dynamics simulations is to use a model which is sufficiently detailed to reproduce the important physical aspects faithfully, and yet not so detailed that the calculations become impractical [HE88]. Hence, the best choice of model depends on the target application physical length and time scales. In the remainder of this section, representative examples of plasma simulation models are briefly presented.

One of the models used more often is the collisionless plasma model, which provides a detailed description of the motions of plasma particles in self-consistent electromagnetic fields [Eas93]. The Eulerian-Lagrangian approach is the pre-eminent method used for collisionless plasmas. The particles' attributes (velocity and position) are obtained through Newtonian motion equations whose driving terms are given by the Poisson equation, arguably the most important of the field equations [HE88], given by:

$$-\nabla^2\phi = \frac{\rho}{\varepsilon_0}, \tag{4}$$

where $\nabla^2\phi$ is the Laplacian of the electrostatic potential, $\rho$ is the charge density function, and $\varepsilon_0$ is the permissivity of free space.

The "particles" in a collisionless plasma simulation correspond to millions of physical charges. Provided that the physical phenomena have wavelengths that are long compared with the average charge spacings, and time scales that are short compared with the time for the graininess to have significant effect, this description gives an accurate representation and leads to the concept of computational "superparticle" [HE88]. The graininess introduced by the paucity of superparticles is minimized by smoothing the short-range forces. Superparticles can be interpreted as finite-sized clouds of electrons, where the position of a superparticle is the center of mass of the clouds, and their velocities represent the mean velocities of the clouds. Alternatively, superparticles can be portrayed as blobs of incompressible phase fluid moving in (position-velocity) phase space [HE88].

In a hybrid Eulerian-Lagrangian formulation, the field and particle quantities are usually defined on different grids. To obtain the charge density at mesh points from the distribution of particles, one can allocate the particle charges based on a CIC (cloud-in-cell) [BL91] charge assignment scheme: the charge density $\rho$ at a grid point $G$ is given by the sum of weighted charges of the particle clouds in the cells surrounding $G$ divided by the cell area. Alternatively, the charges can be assigned by linear interpolation to the nearest grid points, a scheme known as PIC (particle-in-cell) [BL91].

The lengths and time scales in a collisionless plasma model are determined by the collisionless plasma frequency and Debye length (Section 2.1). The model is valid for time scales shorter than the collision time, which is increased by the smoothing of short-range interaction [HE88]. This type of model is usually applied to the investigation of high temperature and dilute plasmas [HE88], as well as applications involving basic plasma processes, instability growth and saturation, and turbulence effects [Eas93].

Incidentally, the modeling of spiral galaxies of stars is another example of collisionless simulation, where the superparticles represent millions of real stars [HE88]. Although stars are not charged, they qualitatively behave like particles in a plasma, and plasma kinetic theory has been used to simulate the development of these galaxies [Che84]. Length and time scales are determined by the dimensions and motion of the spiral arm structures. Collisional effects are made small by smoothing the force of interaction at short range, and by having a large number of superparticles within the range of smoothing [HE88].

For plasma phenomena where collisions are not negligible, a kinetic model is required [Eas93]. In this model, the equations of motion incorporate collision terms which involve gradients in velocity. These gradients are evaluated either using Monte Carlo methods for scattering particles or a velocity space mesh. The usual applications for this type of model are beam-plasma heating and wave-plasma heating [Eas93].

The longest time scale plasma model is the MHD equilibrium [Eas93]. Dynamics are reduced to force balance, and fields are given by magnetostatics. A variation of this model is the nonlinear time-dependent MHD model, which assumes simple physics and complex geometries. It has important applications in science and engineering, such as solar flares, magnetic substorms, MHD dynamo and field reversal, and disruptions in tokamaks.

## 3. Rendering Approaches and Applications

Different criteria can be used to group the approaches used to render plasma phenomena manifestations. The classification used in this report is based on the demands placed on the applications with respect to the degree of realism. Using this criterion, we divide the approaches into two groups. The first group involves rendering applications whose main goal is to depict specific physical characteristics or effect of a given phenomenon. For these applications, the central aspect is the physical information provided by the images. We loosely designate the rendering approaches used in these applications as *illustrative*. The second group involves applications that aim to provide visually plausible representation of plasma phenomena, *i.e.*, applications that incorporate realism to some extent. The resulting visual representations may vary from being just believable to being physically correct (providing the same visual stimulation as the actual phenomena [Fer03]) or photo-realistic (inducing the same visual response as the actual phenomena [Fer03]). We loosely designate the rendering approaches used in these applications as *realistic*.

### 3.1. Illustrative Representations

Numerical simulations in the physical sciences can be complex to the point of being almost incomprehensible without visual representation [UBR*87]. Accordingly, the advances in the field of computer graphics are no longer ignored by the physical sciences community [UBR*87], which is taking advantage of the available rendering tools not only to assist the interpretation and analysis of simulation data, but also for educational and public outreach purposes [Nat03]. In the case of plasma phenomena, these tools are used to depict parameters associated with its visible manifestations (*e.g.*, the visible light emissions caused by plasma particles) as well as to delineate its invisible manifestations (*e.g.*, the coupling of plasma motion with magnetic fields). In this section, we highlight relevant applications of illustrative representations of plasma phenomena manifestations.

#### 3.1.1. Controlled Fusion

One of the most fundamental issues in controlled fusion research is the understanding of plasma turbulence occurring in tokamaks (Section 2.2), which cause particles and energy to escape the confining magnetic fields. Predictive models of such phenomena can reduce the uncertainties in the design of tokamaks and lead to better confinement operating regimes, which, in turn, can reduce the size and costs of fusion reactors [PCS95, Tan02].

Parker and Cummings [PCS95] developed a three-dimensional toroidal gyrokinetic particle model to investigate these phenomena. Gyrokinetic equations are analogous to Maxwell's equations and Newton's force law. In order to interpret the data resulting from their simulation they used visualization tools, such as AVS and Iris Explorer [BDG*03], as well as isosurface rendering techniques and animations.

Schussman *et at.* [SMSE00] have developed a software to interactively present scientists with three-dimensional views of tokamak field lines using simple graphics techniques. The lines are rendered using the Phong illumination model to enhance the perception of their curvature. In addition, the lines are rendered as if they have a dark halo around them. This helps to distinguish which lines are closer to the viewer since these halos obstruct the view of any lines passing behind them. In order to achieve interactive rates, they explore hardware texturing and display lists.

McKee *et al.* [MFF02] used two-dimensional measurements of density fluctuations in a tokamak to generate images and animation sequences of plasma turbulence. Turbulence images are used not only in the visualization of turbulence structures, but also in the measurement of shear flows and the turbulence velocity field. The images produced by McKee *et al.* [MFF02] describe two-dimensional density fluctuation which are color coded to represent regions of equilibrium and regions of positive and negative fluctuations.

Chen *et al.* [CJP02] used a low-cost high-performance stereoscopic visualization system developed by Jones *et al.* [JPK01] to perform three-dimensional gyrokinetic toroidal simulations of tokamak plasma turbulences. This system uses volume rendering techniques to create visual representations for simulation data sets, and OpenDX, an open source visualization software [TBF00], as its visual analysis tool. The stereo images produced in their relative low cost hardware set-up are projected and superimposed onto a lenticular screen to create the illusion of depth to a user wearing polarizing glasses.

In addition ot these works described in the literature, several governmental agencies and research centers are making use of visualization tools to produce illustrative renderings of plasma phenomena that occur in controlled fusion facilities. The reader interested in more examples of such applications is referred to the reviews by Tang [Tay01] and NRC [Nat95].

#### 3.1.2. Solar Plasma Interactions with Magnetospheres

Earth's magnetosphere and ionosphere formed the historical starting point for space physics research. In the past

**Figure 10:** *Frames of an animation showing plasmasphere's changes due to a solar storm that occurred in 2003. Top) Plasmasphere before the full impact. Bottom) A portion of the plasmasphere convects out to the magnetopause (represented as a grey, semi-transparent surface) where it terminates. Courtesy of NASA/Goddard Space Flight Center, Scientific Visualization Studio.*

four decades they have remained an important focus for scientific studies not only because they constitute the human space environment, but also because their study can provide important insights about the magnetosphere and ionosphere of other planetary bodies in the solar system and about basic space plasma phenomena that occur in remote and inaccessible regions in the Universe [Nat03]. These studies include numerous space, ground-based investigations as well as computational simulations. These simulations usually employ standard mathematical visualization packages in which simple color code based schemes are applied to represent physical variables such as thermal pressure distribution, current density, plasma density, plasma temperature and energy levels [AML*04, EWCB04, FZP03, LSL*04, GPZ*04].

In 1983, Blinn and Wolf [UBR*87] produced a film entitled "Jupiter's Magnetosphere: The Movie". In this film representations of spacecraft observations as well as analytic models of the plasma and magnetic fields in the Jovian system were employed to depict the three-dimensional morphology and dynamical structure of Jupiter's magnetosphere. To the best of our knowledge, this film represents the first plasma related simulation reported in the graphics literature.

Due to the broad importance of magnetic fields in large-scale plasma dynamics, the development of a first-principles understanding of the physical mechanisms that control the generation and dissipation of magnetic fields has become a fundamental goal in plasma science [Nat04]. The release of magnetic energy is often observed to occur in processes that produce intense plasma heating, high-speed-flows, and fast particles such as solar flares and CMEs (Section 2.2). Magnetic reconnection, a process in which oppositely directed magnetic field components rapidly merge to release the stored magnetic energy, has been identified as the dominant mechanism for dissipating magnetic energy [Nat04]. Illustrative rendering techniques have also been used to produce two and three-dimensional representations of these phenomena using standard mathematical visualization packages and color code schemes [SDRD99, GPZ*04, OPL*04].

In 1997, for the first time ever, the satellites of the International Solar-Terrestrial Physics (ISTP) Observatory have tracked a solar eruption all the way, from a CME expelled from the Sun, through interplanetary space, until it hit the Earth's magnetic environment, causing there violent disturbances and spectacular auroral displays. The initial expulsion occurred on the Sun on January 6, 1997, and a resulting magnetic cloud hit the Earth on January 10. Goodrich *et al.* [GLW*98] performed MHD simulations of the resulting geomagnetic storm. The visual simulations, also based on the use of standard mathematical visualization packages and color code schemes, were validated by ground-based and geosynchronous observations, and eventually were used by the Space Plasma Physics Group and the Advanced Visualization Laboratory at the University of Maryland to generate a video (about 10 minutes in length) depicting in significant detail the impact of this CME on the Earth's magnetosphere.

Besides academic institutions, governmental agencies also support visualization initiatives to facilitate scientific inquiry and public outreach. For example, the Scientific Visualization Group at NASA Goddard Space Flight Center, has produced several illustrative visualizations describing solar plasma interactions with the Earth's magnetosphere, which oftentimes incorporate actual measured data. Figure 10 shows frames of an animation showing the effects of a 2003 solar storm on the Earth's plasmasphere, a region of cold plasma which co-rotates with the Earth, carried by the magnetic field lines. During the 2003 event, the electrical fields created by the storm convected some of the cold plasma out to the outer border of the Earth's magnetosphere, the magnetopause, and reduced the size of the cold plasma region near the Earth. For this animation, the three-dimensional structure of the plasmasphere was constructed from the data collected by Extreme Ultraviolet Imager (EUV) instrument on board the NASA Imager for Magnetopause-to-Aurora Global Exploration (IMAGE) satellite.

Recently, Goodrich *et al.* [GSL*04] have proposed a simulation code coupling strategy for the Center for Integrated

Space Weather Modeling (CISM) and the NASA Living With a Star (LWS) program (aimed at the deployment of a fleet of spacecraft to probe the solar, near Earth and ionosphere conditions), in which global and local simulation models are integrated. The former address the corona, the heliosphere (a bubble of magnetized plasma enclosed by current sheets and encompassing the entire solar system) and the Earth's magnetosphere and ionosphere, whereas the latter address processes such as magnetic reconnection. One may expect a similar strategy being applied to supporting rendering tools, which would have to fulfill the same requirements, namely efficient transmission of information among codes, interpolation of grid quantities, translation of physical variables between codes with different physical models, and control mechanisms to synchronize the interaction of codes.

### 3.1.3. Astrophysical Events

Ljung [Lju00] developed a particle data visualizer (PDV) for interactive real-time rendering and animation of PIC simulation data. The system, implemented using OpenGL [WNDS99], supports several rendering and visualization techniques: Ribbon graph for the visualization of one-dimensional scalar functions, two-dimensional height fields, volume rendering of particles densities, and the rendering of individual particles. The last two techniques were used in a case study [LDAY00, DLYM02] aimed at the investigation of instabilities associated to plasma surfatron (Section 2.2), a process of electron acceleration observed in Nature (*e.g.*, astrophysical shocks [DLYM00, MDY*01]) and in laboratory (*e.g.*, particle accelerators [Jos06]). In this case study, the focus was the simulation of wave-particle interactions in a magnetized plasma acting on specific parts of the electron phase-space (Figure 11). The electron phase space was visualized by distributing the simulation electrons over an array representing phase space density, and volume rendering this array. The particles densities were rendered using a volume slicing technique which uses textures and polygons to sample a volume and render it. The computer architecture used in this case study, namely a Silicon Graphics InfiniteReality engine [MBDM97], allows a data volume to be directly downloaded to a graphics system as a three-dimensional texture. The images are rendered by drawing polygons (intersecting the volume) in a back to front order and composing them with blending. Due to hardware constraints, however, they had to consider only a limited resolution of phase space for the volume rendering and only a subset of the simulation particles in the rendering of electrons as points [LDY02]. In order to provide a depth cue during the rendering of individual particles, the OpenGL fog supported feature was used to fade electrons that are farther away. The implementation framework used in the PDV system also enables the use of stereo visualization techniques.

One of the great challenges in astrophysics is to elucidate the structure of neutron stars [Sho03]. The powerful gravitational attraction of a neutron star extremely dense

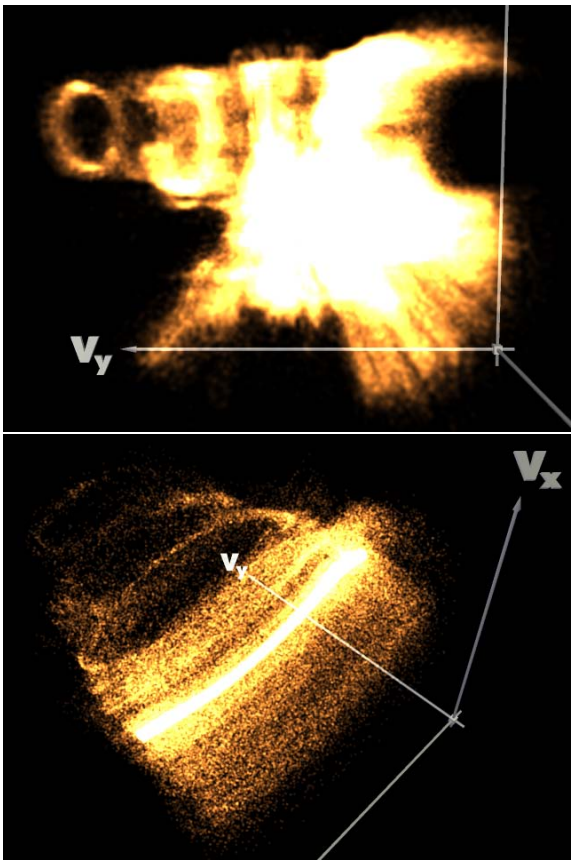


**Figure 11:** *Computer generated images showing electron phase-space distributions and the emergence of plasma surfatron. The higher the intensity, the larger the number of electrons. Top) volume rendering of electron densities. Bottom) rendering of individual electrons as points. Courtesy of P. Ljung, M. Dieckmann and A. Ynnerman.*

body allows only neutrinos and high-energy photons to escape, making it detectable only by X-ray measurement instruments [Las99]. Recently, Price and Rosswog [PR06] presented a simulation of neutron star mergers that took magnetic fields into account for the first time. Figure 12 show frames of an animation sequence depicting two neutron stars merging into a single object, with excess angular momentum being transported outward in spiral arms that quickly spread into a thick accretion disk around the central object. A shear layer is form when the stars coalesce, and even small perturbations in this layer cause it to curl up into vortex rolls due to Kelvin-Helmholtz instability [LH68], which often accompanies flows where shear is present. The amplification of the magnetic fields occurs on a time scale of $1ms$. The three-dimensional simulations were performed using a SPH scheme (Section 2.4), and the animation frames were rendered using SUPERSPHPLOT [Pri06], a public

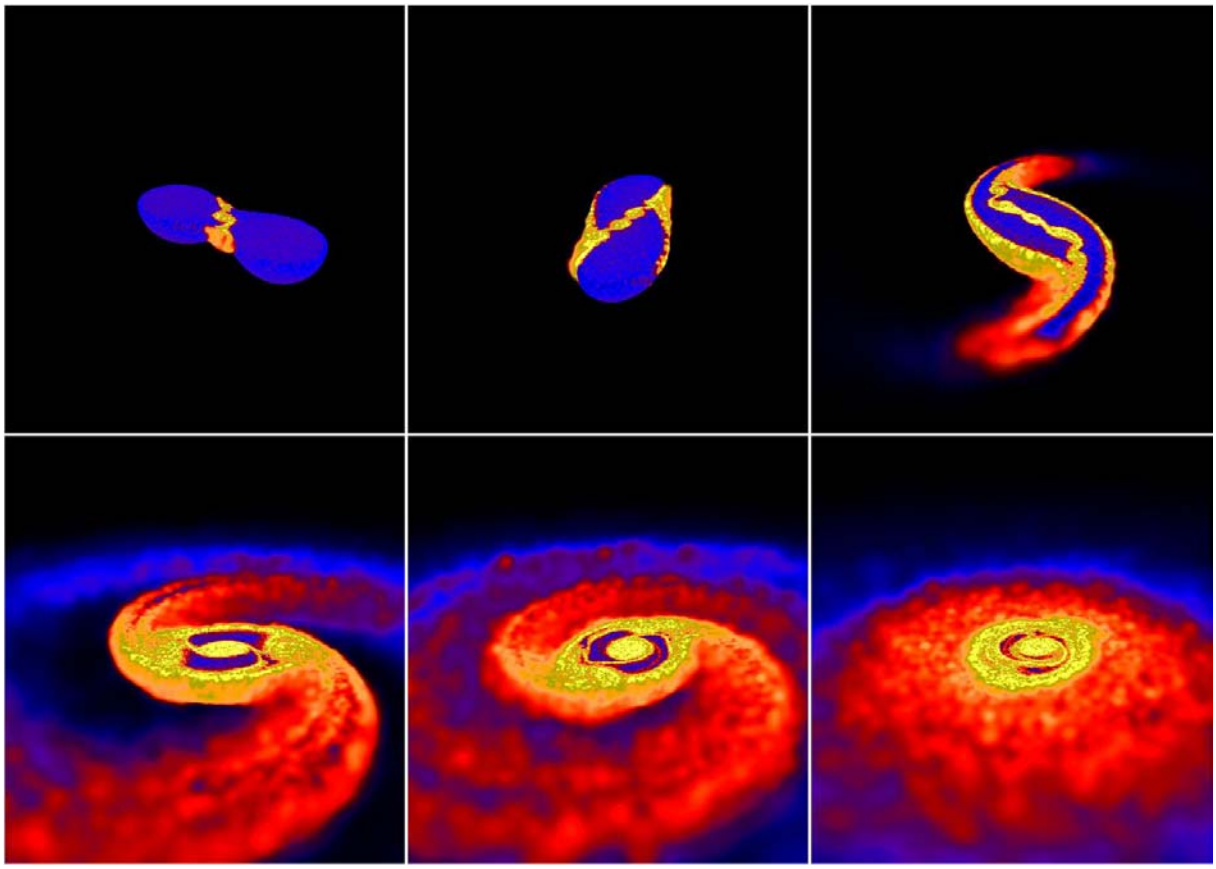

**Figure 12:** *Frames of an animation depicting the results of a coalescence simulation of two magnetized neutron stars. It highlights the magnetic field strengths in the accretion disk material at and below the orbital plane. The stars move gradually to each other, merge and finally form a hot torus. The whole process (from left to right, top to bottom) takes 11.34ms. Courtesy of D.J. Price and S. Rosswog.*

domain software specifically designed for the visualization of SPH output. This visualization tool, written in Fortran 90, utilizes the public domain PGPLOT [Pea97] graphics subroutine library to do the actual plotting. The 1.5 version of SUPERSPHPLOT includes an option for the three-dimensional surface rendering of SPH data which was used to render the images presented in Figures 1 and 12. It consists in producing a visualization of the surface of a data set by performing a ray-trace through the SPH particles, with the density distribution giving the optical depth, and the rendered quantity (in this case the strength of the magnetic fields) providing the reference for the colour coding scheme. Thus low density regions will be transparent whilst high density regions will be optically thick, and therefore opaque [Pri06].

Finding evidence of the existence of black holes represents another great challenge in astrophysics [Las99]. The best hope for astrophysicists has been to find a black hole in a binary system. However, to differentiate a neutron star from a black hole, astronomers have to investigate the pattern in which the accompanying accretion disk gives off radiation to deduce which type of object is present [Las99]. Such pattern is associated with the accretion flow, whose study remains a very active field of research. For example, Armitage and Reynolds [AR06] used global MHD simulations to investigate the temporal variability of accretion disks around black holes. The models used in the simulations are three-dimensional, and the equations are solved using a numerical MHD simulation code. They calculated the predicted emission that would be seen by an observer using a relativistic ray tracing method that accounts for relativistic effects of beaming, or headlight effect (charged particles moving at a significant fraction of the speed of light will emit electromagnetic radiation in a narrow beam in the direction of motion, which may modify the apparent luminosity of an astrophysical object since as the particles' speed approach the speed of light, the beam gets narrower [OC96]), light bend-

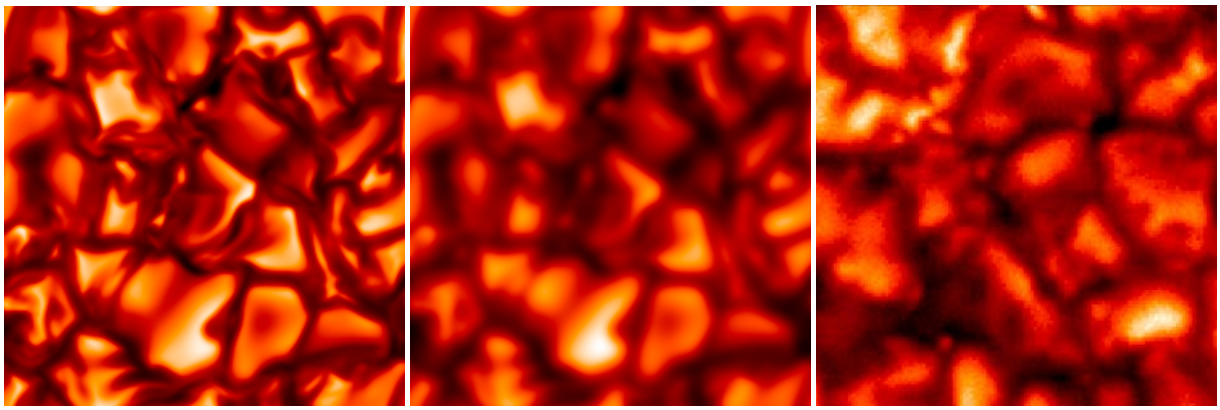

**Figure 13:** *Images showing a simulation of granulation (left), the same image folded with a point spread function to compensate for atmospheric scattering (middle), and an actual observation of the phenomenon provided by the Swedish Solar Observatory and Lockheed-Martin Solar and Astrophysics Laboratory (right). Courtesy of R. Stein and A. Nordlund.*

ing and K-correction (used to transform observed measurements at a redshift z, into a standard measurement at redshift zero, the rest-frame [Sho03]). Their simulation results were used to produce frames for an animation sequence depicting a turbulent accretion disk surrounding a non-rotating (Schwarzschild) black hole [OC96] as seen by a distant observer. During the sequence, the camera moves from a face-on view of the disk to an almost edge-on angle. The relativistic effects of beaming and light bending become increasingly apparent at higher inclinations. In order to generate the animation frames and compute the light curve, they calculated the mapping between the rest frame emission and that seen by a distant observer (the "transfer function") using the ray tracing method mentioned above. Their calculations of light curve and power spectra also accounted for the differing time of flight of photons from different regions of the accretion disk.

### 3.2. Realistic Representations

The qualitative and quantitative insights obtained from numerical simulations and subsequent realistic visualizations can inspire new ways to looking at the phenomena under study [NSB96]. Accordingly, many studies related to plasma phenomena are making use of realistic visual representations. Such representations of plasma phenomena manifestations have been also developed for entertainment and educational applications such as movies and planetarium shows. In this section, we highlight relevant and original work by physical sciences and computer graphics researchers involving realistic representations of plasma phenomena manifestations.

#### 3.2.1. Solar Phenomena

Interest in solar science is currently increasing due to significant advances in observations satellites and Earth-based telescopes, and due to the realization that the behavior of the Sun has significant effects on the climate of the Earth [Sup04]. However, as appropriately stated by Stein [Sup04], photographs and data 'tell us what's there, but not why it is there". Consequently new theories about several solar plasma phenomena are being developed using computer modeling in conjunction with realistic visual representations of these phenomena, which are often validated through comparisons with actual observed data.

Among these phenomena we can highlight the formation of granules, short lived cells of plasma that carry heat to the surface through convection. When the base of the solar photosphere is observed, it appears as a patchwork of bright and dark regions, the granules, that are constantly changing, with individual granules appearing and then disappearing [OC96]. This patchwork structure is known as granulation. Stein and Nordlund [SN00] have performed three-dimensional realistic visual simulations of this phenomenon, and made comparisons between simulated and observed granulation (Figure 13). The emergent continuum radiation in the granulation simulation showed good agreement with the observed solar intensity when the simulation results are smoothed with a modulation transfer function to account for atmospheric scattering. They employed a numerical MHD simulation code to model the convection processes, and the results of their simulations were used to produced the images of the phenomenon using IDL (Interactive Data Language) [Bow05], a proprietary software systems employed by scientists and engineers in the analysis and visualization of data sets. Besides its connection with radiative energy exchange processes, this phenomenon is also associated with magnetic processes. Hence, its simulation can also be used to make such processes "visible".

Coronal loops (Section 2.2) are also examples of solar plasma phenomena that can be used to study magneto-

convection processes. Gudiksen and Nordlund [GN02] have performed three-dimensional simulations of coronal loops using a MHD numerical approach, and the results of their simulations were used to produce animations of the phenomenon also using IDL (Interactive Data Language) [Bow05]. The densities of the simulated loops were consistent with observations made by TRACE. Figure 14 presents one of the simulations performed by Gudiksen and Nordlund. It uses a "false" color approach to represent the ultraviolet (195*nm*) emissions where white represents the brightest ultraviolet emission. The simulations were performed on a grid with 150 points in each direction, making the resolution of the images only 150 by 150 pixels. Higher resolution images were then made from interpolation between the values generated by the simulation [Gud06].

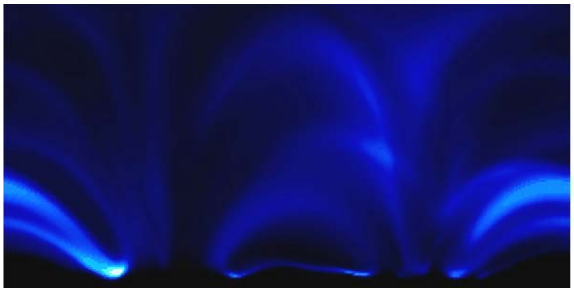

**Figure 14:** *Image of coronal loops emulating TRACE observations at* 195*nm. Courtesy of B. Gudiksen and A. Nordlund.*

### 3.2.2. Lightning Discharges

The rendering of lightning discharges (Section 2.2) has been addressed in several works in computer graphics [RW94, Kru99, Gla00, DYN01, SFMC01, KL04, VR06]. However, to the best of our knowledge, there has been no attempt to directly simulate plasma processes for the purpose of rendering lightning discharges.

The first computer graphics model specifically designed for the rendering of lightning was proposed by Reed and Wyvil [RW94]. Their model was based on the empirical observation that most cloud-to-ground lightning branches deviate by an average of $16^\circ$ from parent branches. Accordingly, the lightning channel segments were generated as a set of randomly rotated line segments whose angles were uniformly distributed around $16^\circ$. They used a ray tracing algorithm and an heuristic shading function to render lightning strokes. This function incorporates a exponential decaying term to account for glowing effects observed in photographs of lightning, and it varies according to the shortest distance between a light segment being rendered and the point of intersection between a ray and the plane containing the segment. The model proposed by Reed and Wyvil was used to generate believable images of cloud-to-ground lightning which presented a good qualitative agreement with photographs of the real lightning discharges. Dobashi *et al.* [DYN01] extended the work by Reed and Wyvill through the incorporation of atmospheric scattering formulation based on the integration of intensity contributions along the viewing ray using a simple cosine-based scattering phase function.

Most computer graphics models of lightning focus on the shape of the lightning (plasma) channel. Kruszewski [Kru99] proposed a parametric model for lightning strokes based on random binary tree results from probability theory. Glassner [Gla00] proposed yet another stochastic method model based on data derived from a set of 40 digitized lightning channels collected for the Apollo space program from lightning photographs. It consists in modeling the lightning channel in two passes. The first pass creates the large scale structure, and the second pass adds the small scale detail (tortuosity).

Sosorbaram *et al.* [SFMC01] presented the first physically-based model to simulate electric discharges, which can be used in the rendering of cloud-to-ground and cloud-to-cloud lightning. It consists in placing charges and defining electric potentials over a discretized volume, and computing the pattern of the lightning channel using the dielectric breakdown model (DBM) [NPW84]. The lightning channel for cloud-to-ground lightning is performed using a simple volume rendering technique based on the use of three-dimensional textures. For the cloud-to-cloud lightning, a step leader is represented by a number of light sources.

The physically-based framework for the rendering of lightning discharges proposed by Kim and Lin [KL04] also applies the DBM to simulate the pattern of the lightning (plasma) channel as a series of thin line segments. They hypothesized that humans perceive that a lightning stroke is thicker than the actual thin plasma channel because the brighter portions of the glow exceed the range perceptible by the human visual system, and as a result these portions merge into what is perceived as a thicker bolt. To achieve the same effect, they applied an atmospheric point spread function (APSF) on the two-dimensional rendering of the line segments. This function consists in a series expansion of the Henyey-Greenstein scattering phase function [HG41]. According to Kim and Lin, if the brightness of the plasma channel is set properly, the APSF should produce luminance values that exceed the range of the display device, creating the expected thick bolt. The model proposed by Kim and Lin also allows the generation of believable images of lightning discharges which present a good qualitative agreement with photographs of actual phenomena.

Recently, Varsa and Rokne [Var04, VR06] presented the first computer graphics simulation of ball lightning. To date, the ball lightning theories presented in the scientific literature can explain only a fraction of the reported displays of this elusive phenomenon [Ste00]. However, a large num-

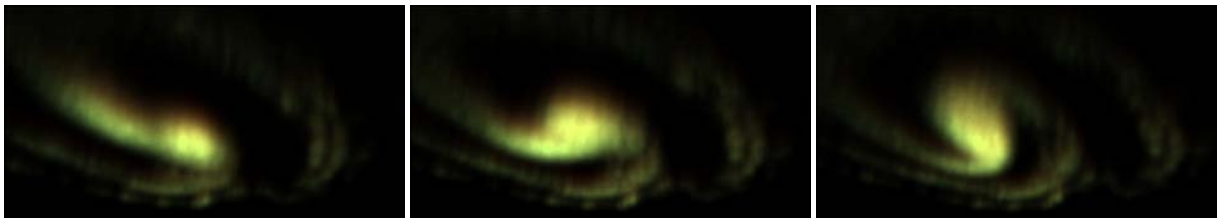

**Figure 15:** *Frames of an animation sequence simulating an auroral spiral (surge) formation.*

ber of models suggest that the plasma is the source of the phenomenon luminescence [GR95, Ste00]. Varsa and Rokne also assumed that ball lightning is a form of contained plasma, and used a physically-based model [Gaí89, Gaí91] to approximate its motion and deformation patterns. The rendering itself was performed using particle systems [Ree83], where the particles are in fact superparticles (Section 2.4) representing independent units of light emitting plasma.

### 3.2.3. Aurorae

Baranoski *et al.* [BRS*00, BRS*03] presented the first physically-based algorithm for the three-dimensional visualization of auroral displays. Their algorithm accounts for auroral visual features such as their characteristic spectral and intensity variation. Their work, however, did not take into account the electromagnetic instabilities responsible for the time varying behavior of the aurorae, which was addressed in a subsequent paper [BWRB05] examined later. Nonetheless, it provided an accurate framework for the rendering of realistic auroral images (Figure 2).

Aurorae are view dependent phenomena, *i.e.*, the apparent surface brightness of an aurora is proportional to the integrated emission per unit volume along the line of sight. Baranoski *et al.* [BRS*00, BRS*03] used a forward mapping, or splatting, approach to map auroral emissions to the screen plane [Wes91]. The emissions mapped to the screen plane are then scaled according to auroral spectral emission and intensity profiles [BE94, VK20], which correlate with the height of the emission point.

The different lifetimes of transition states in auroral emissions cause the photon emissions to occur in distinct volumes around the principal direction of emission (Section 2.3). Statistically, the intensity contribution of the emitted photons spreads radially around the propagation direction, and follows a Gaussian distribution along that dimension [BSBD91, BS93]. Hence, in order to simulate this distribution of auroral emissions, Baranoski *et al.* [BRS*00, BRS*03] convolved the image with a color-dependent Gaussian low-pass filter [Wes91].

An auroral display also exhibits global temporal variations captured in photographs as blurred forms, due to finite exposure times. To account for this global blurring effect, *i.e.*, to facilitate the comparison with photographs of auroral displays, they performed a convolution using a temporal low-pass filter [Cas96]. The longer the sampled-window is in time, the blurrier the results, similar to the effects captured in real photographs with longer exposure times.

Later on, Baranoski *et al.* [BWRB05] presented a physically-based model for the three-dimensional visual simulation of auroral dynamics. The model employs a complete multigrid [CW00] PDE simulation of the electromagnetic interactions between auroral electrons. It allows an accurate and efficient visualization of auroral phenomena at different spatio-temporal scales. Their work resulted in the first physically-based three-dimensional visual simulations of these phenomena published in the scientific literature.

Instead of tracking the around $10^{12}$ individual plasma particles that cause auroral phenomena, they followed the path of superparticles (Section 2.4) referred to as beams of electrons. The key stage of their modeling framework is the simulation of the warping process, which changes the perpendicular velocity (with respect to the Earth's magnetic field lines) and the position of the electron beams. The mathematics of this process can be described by an electro-magnetic version of the Kelvin-Helmholtz instability [Hal76, Hal81, LH68, PFK01], in which the potential (Poisson) equation and the electron beam perpendicular velocity equation formed a coupled continuous superparticle system. This system is solved using and a hybrid Eulerian-Lagrangian approach (Section 2.4), where an Eulerian grid is used for the potential equation (with superparticles charges allocated using the CIC method and the PDEs solved using a FD method), and a Lagrangian grid is used for the velocity equation.

During their descending trajectories, the electron beams may be deflected several times due to collisions with atmospheric constituents. Light emissions may occur at these deflection points causing the auroral displays. These emissions are mapped to the screen plane of a virtual camera using the algorithm previously described [BRS*00, BRS*03]. The resulting images, which exhibited good qualitative agreement with photographs of auroral display, were used to produce animations illustrating auroral motions and sharp changes at different spatio-temporal scales such as auroral "dancing" rays and auroral spirals (Figure 15).

#### 3.2.4. Space Nebulae

Nadeau *et al.* [NGN*01] used volume rendering techniques to create a three-dimensional visualization framework for the emission nebula Orion. The nebula's thin ionization layer, which is responsible for its visible glow, was modeled using a three-dimensional model of the nebula's apparent surface derived by Zheng and Dell [WO95] from infrared and visible light observations. This model is imported into a volume scene graph-based visualization system (a hierarchical organization of shapes and groups defining shape content [Nad00]) which uses procedural volume modeling to simulate the nebula's emissive plasma layers. Additional scene graphs were used to model proplyds, *i.e.*, circumstellar disks of dust and gas surrounding protostars (stars in the making or pre-nuclear-burning astrophysical objects [OC96]), which appear as fuzzy blobs even when seen through the Hubble Space Telescope.

In their simulation of the Orion Nebula, Nadeau *et al.* [NGN*01] employed a texture mapping approach to represent its spectral variations, *i.e.*, they used an image provided by the Hubble telescope which encodes both color and intensity. To give the nebula its color and brightness, the Hubble image was projected through the volume along a vector from Earth. The image was processed first to reduce its red content, correcting for the reddening effects of intervening material between Earth and the nebula. Because stars and shock fronts were added later, these were painted out of the Hubble image.

Although the Orion Nebula complex provides a unique laboratory for the research of plasma phenomena such as outflows, jets and shocks [OB00], the main purpose of the framework described above was educational. It was used in the production of a 2*min* fly-through animation of the Orion Nebula (Figure 16) for the Hayden Planetarium (San Diego, C.A., U.S.A.).

Magnor *it et al.* [MKHD05] used a constraint inverse volume rendering algorithm [MKHD04] to automatically recover the three-dimensional distribution of the ionized gas in planetary nebulae. This algorithm relies on three assumptions: most planetary nebulae exhibit a symmetry axis, scattering and absorption are negligible at visible wavelengths, and the project appearance of planetary nebulae is essentially orthographic since they span only a few arc minutes in the sky. The algorithm uses a planetary nebula model which consists of a two-dimensional density map whose entries represent axisymmetric emission density values. This map is aligned with the symmetry axis of the nebula, and the algorithm determines all map entry values such that the corresponding rendered image, obtained by rotating the emission density map around the symmetry axis and integrating emission along the line of sight, matches the nebula photograph. The emission map entries and the two orientation angles of the symmetry axis represent the model parameters that need to be optimized. The integration of the emissions

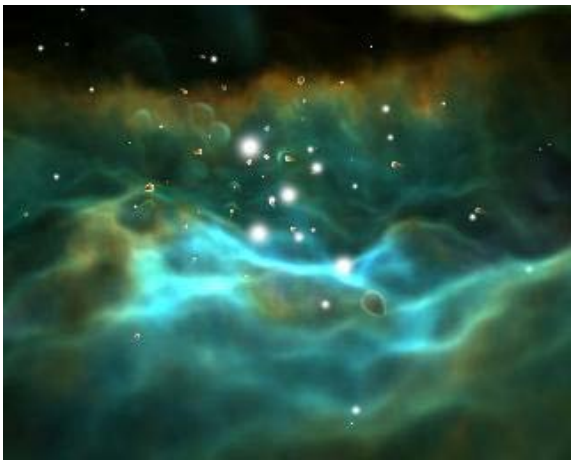

**Figure 16:** *Frame of an animation depicting the Orion Nebula. Courtesy of D.R. Nadeau, J.D. Genetti, S. Napear, B. Pailthorpe, C. Emmart, E. Wesselak and D. Davidson.*

along the line of sight is accomplished using volume rendering techniques implemented in graphics hardware. From the reconstructed spatial emission distribution, the nebulae can be rendered from arbitrary perspective (Figure 17). Planetary nebulae images rendered using this approach can also be used in educational and public outreach applications.

It is worth noting that reflection nebulae have also been object of investigations by computer graphics researchers [MHLH05]. However, they are not luminescent plasmas as emission nebulae, *i.e.*, they are visible due to the scattering of light (emanating from nearby bright star(s)) by carbon dust particles) [Mal89, Mal94].

## 4. Challenges and Trade-Offs

Despite the recent developments on the visual representation of plasma phenomena, computer graphics and physical sciences researchers continue to look for more effective rendering solutions. In this quest, they face similar technical challenges and trade-offs, which are outlined in this section and illustrated through examples related to the applications described in the previous section.

### 4.1. Data Availability

The simulation of natural phenomena involving shear and fluid flow has been attracting the attention of computer graphics researchers for many years. Since the plasma instability responsible for the stochastic and complex nature of various phenomena (*e.g.*, formation of a neutron star accretion disk and auroral shape changes) is similar to the Kelvin-Helmholtz instability for sheared fluids [Taj89], one might suggest that models used for fluids, such as smoke and water, could be also applied to the simulation of plasma phenomena

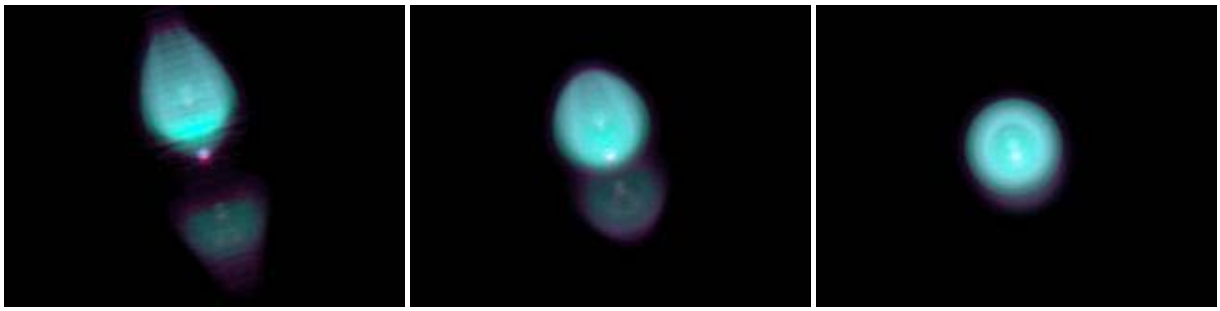

**Figure 17:** *Images depicting the planetary nebulae M1-92 as it would look at inclination angles of* $85^\circ$, $35^\circ$, *and* $10^\circ$ *(left to right). Courtesy of M. Magnor, G. Kindlmann, C. Hansen and N. Duric.*

(Section 2.4). Although it would be possible to obtain similar visual representations using such models, this approach would not lead to predictable results since the plasma simulations would not be controlled by plasma physically meaningful parameters, *i.e.*, the choice of parameters would be arbitrary and therefore difficult to be duplicated by different users.

Predictability is a required attribute for scientific applications. After all, what's the value of a theory or a model if their outcomes cannot be reproduced? One might argue, however, that such a control would not be necessary if the goal is just to generate believable images of a given phenomena. Again, the reproducibility aspect comes to play. Computer graphics researchers and developers, including those working in the games and entertainment industries, can certainly benefit from being able to automatically generate realistic images through the use of predictive models.

The use of a model based on the current physical understanding of the phenomena is just the first step, however. Predictive simulations, require both theory and data, and one has limited value without the other. This data can be classified into two main categories: characterization data and evaluation data. The former is required as input for the model, the latter is used in evaluation procedures which are examined in the next section.

In the case of plasma phenomena, even though many resources are being invested in their study (Section 2.2), there is still a certain scarcity of fundamental data. For example, since the aurora is characterized by a storm-like behavior, the variations of spectral ratios and intensities according to the auroral heights are given in the literature as average values, which are themselves limited to three wavelengths. Although these spectral and intensity profiles are a good approximation for the vertical emission profile [RB67], it would be necessary to account for several other weaker light emissions at other wavelengths across the visible spectrum to fully reproduce the variety of colors that can be observed in auroral displays (Section 2.3). To the best of our knowledge, such data is not readily available in the literature.

### 4.2. Evaluation Approaches

Depending on the target application, different evaluation approaches can be used to determine the effectivity of a rendering framework. For instance, if the goal is the synthesis of believable images of phenomena commonly observed in Nature (*e.g.* lightning), a simple visual inspection of the resulting images may be used to indicate whether or not the goal was achieved. When the main purpose is to convey or highlight some specific information about the phenomena (*e.g.* the illustration of electron phase-space distributions), finding the appropriate methodology to determine the degree of fidelity of a given visual representation is usually a difficult task since it involves perception and context issues, such as the observer's prior knowledge about the phenomena and its underlying physical principles, that may vary from one individual to another.

Realistic representations aimed at scientific applications need to provide either quantitative or qualitative evidence of their accuracy and predictability. Otherwise they cannot be reliably employed in scientific investigations. Usually quantitative evidence is obtained through measurements. The quasi-stochastic nature of several visual manifestations of plasma phenomena along with inherent measurement difficulties reduces the viability of a quantitative analysis of their visual simulations, often leading to a qualitative verification approach. Qualitative evidence is usually obtained through comparisons with actual observations of the phenomena or existing records such as photographs and videos. The problem is that usually these records do not provide an accurate representation of the actual phenomena. For example, the appearance of solar granulation (Section 3.2.1) observed from space differs from a ground-based telescope observation subject to the influence of atmospheric scattering. Another example refers to auroral videos and photographs which are usually blurred due to low light conditions and significant exposure times, and for these reasons do not show high frequency features that might be observed by the naked eye. In these situations, physical sciences and computer graphics researchers face the the same question:

should the simulation images, to be published, simply represent the actual phenomena, which may not be easily observed, or should they incorporate external effects (such as the atmospheric scattering accounted for in the granulation simulation and the blur incorporated in the auroral simulation) to facilitate the comparison with photographs?

For scientific or computer graphics applications aiming at predictable results is essential that, whenever feasible, one provides as much evidence as possible to allow others to completely assess the merit of one's contribution. For example, Stein and Nordlund (Section 3.2.1) provided simulation images depicting the granulation phenomenon and the same images folded with a point spread function to compensate for the atmospheric scattering (Figure 13), which were compared with actual photographs of the phenomenon obtained through a ground-based telescope. In addition, they also quantitatively compared the spectrum of simulated and observed granules [SN00].

### 4.3. Accuracy vs. Computational Cost

Predictable models controlled by physically meaningful parameters are usually computational expensive. For example, the simulation of coronal loops presented earlier ran on a supercomputer for about a month, and used CPU power equivalent to more than a year on a very high end desktop (it also needs so much memory that a desktop could not have handled it) [Gud06].

Although, parallel processing techniques can be used to reduce the computational costs of physically-based implementations [BR02, Tan02, Spr05], they will still be more expensive than ad hoc implementations. The crucial question then arises: is accuracy and predictability priorities for the target application? If they are not, the use of ad hoc implementations that produce images that "look good" should be the appropriate choice. Otherwise, one has to accept the intrinsic computational costs of the implementation and look for solutions to mitigate it. Such solutions may go beyond the use of massive parallel processing, which may not be accessible to some researchers, *i.e.*, they may involve the implementation of faster numerical methods and the use of specialized graphics hardware.

### 4.4. Rendering Issues

The last stage in an image synthesis pipeline involves the mapping of the simulated luminance values to luminance values of the output media (*e.g.*, a video display or a print on paper) to produce the final image. As appropriately stated by Greenberg *et al.* [GAL*97], this is an underappreciated, but important component of the rendering process. It needs to take into account the physical characteristics of the output media as well as the perceptual characteristics of the observer and the conditions in which the phenomenon is observed.

The dynamic range (*i.e.*, the ratio between the maximum and minimum luminance values) of actual visual manifestations of plasma manifestations is usually several orders of magnitude higher than the dynamic range of output media. For example, the brightest night auroral displays have a peak luminance value that corresponds to approximately one third of the luminance of full moon light [Eat80]. Although is possible to convert natural occurring luminances into an acceptable image on an output media, the loss of information is usually unavoidable. Although several compression algorithms have been proposed to minimize such loss [DW00], selecting the "best" algorithm is a delicate task, and no single algorithm provides a superior solution under different viewing conditions such as high light level (photopic) scenes (Figure 5) and low light level (scotopic) scenes (Figure 7). Hence, a pragmatic strategy to cope with this problem may involve the implementation of a set of algorithms, with the one actually used chosen according to the phenomenon properties and the viewing conditions.

The visual manifestations of plasma phenomena provide a broad range of spectral information, and it is clearly insufficient to approximate such physical richness with RGB values. Ideally, the spectral information must be preserved as long as possible in the rendering pipeline, and only converted to three dimensions when mapped to an output media [BB03]. This is, however, and open problem in realistic image synthesis. Although, the interplay between the areas of spectral rendering and tone reproduction has been extensively investigated, and a variety of tone reproduction operators have been proposed [DCWP02], the ultimate goal has not been attained yet, namely an efficient spectral color reproduction that provides more accurate color over all possible viewing environments.

## 5. Future Prospects

There are several avenues for future research associated with the rendering of plasma phenomena and their visual manifestations. Future research in this area may involve not only the improvement of the current rendering/simulation frameworks, but also the broadening of their scope of applications. Such an improvement will likely be associated to the challenges and trade-offs outlined in the previous section. Although it may seem that only incremental work is needed, major multidisciplinary efforts will be required to overcome some of the current obstacles such as data scarcity. The broadening of the scope of applications involving rendering of plasma phenomena and their visual manifestations can be assessed by probing some ongoing research projects in fields as diverse as molecular dynamics and cosmology.

Molecular dynamics (MD) refers to a class of simulations that solve Newton's equations of motion for systems of mutually interacting particles [HG05]. MD simulations have proven to be useful tools for researching weakly ionized materials-processing plasma, and the use of molecular

visualization tools incorporating rendering techniques, such as shadowing and depth-cueing, has enhanced the current understanding of newly conducted MD studies of plasma surface interactions. According to Humbird and Graves [HG05], as atomistic simulations become more accurate in reproducing experimental measurements, visual representations will grow increasingly useful in enabling scientists to extract and visualize microscopic details that would otherwise go unnoticed.

Solar and space physics research explores a diverse range of plasma phenomena encountered in our local cosmos, the solar system. Coronal loops, granulation, solar flares, CMEs, solar winds, magnetospheres and aurorae are just a few of the many phenomena unified by the common set of physical principles of plasma physics [Nat04]. In the case of solar science, discoveries made through computer simulations, some of which have been mentioned in this report (Section 3.2.1), lead scientists to look for supporting physical evidence. We remark, however, that despite much progress in the study of these phenomena, many long-standing fundamental questions remain unanswered [Nat04], and their clarification will likely require the use of predictive visual representations of these phenomena.

The simulation and visual representation of plasma processes is also of great mportance for almost every area of astrophysics investigating the complex dynamics of active plasmas and fields that occur throughout the Universe, from atomic scales to galactic scales [Nat04, NGS96]. These investigations will continue to require modeling and rendering at a large extent, as demonstrated by works on the simulation of relativistic extragalactic jets [HMD02] and jets emitted from black holes (Figure 18), whose origins are still object of investigation [SDP04].

Another field of research in which plasma phenomena and their visual representations play an important role is cosmology (the astrophysical study of the origin, evolution and structure of the Universe as a whole [Haw88], *i.e.*, in its totality of physical phenomena in space and time) . The most advanced cosmological simulations are just beginning to incorporate realistic models of galactic winds and the chemical enrichment of the universe [Sim04]. For example, visual representations are being used in studies involving the dynamics of the gaseous intergalactic medium [CTOJ02], the process of star formation [ABN02], and the nature of dark matter [SFW06]. Even the most sophisticated numerical models, however, must apply broad, simplifying assumptions to make the physical simulations computationally tractable. Although these investigations continue to progress, as both the observations and the theory evolve [Sim04], the discrepancies between observations and visual representations of physical phenomena are essential to point the way to further studies that need to be performed.

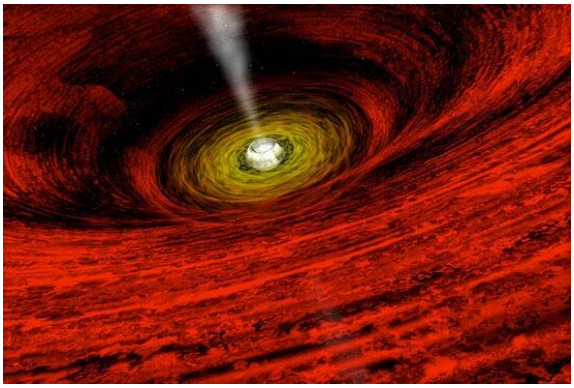

**Figure 18:** *An artist's illustration depicting a black hole surrounded by an accretion disk shown in red and yellow, which acts as fuel for the black hole engine. Power generated by the engine flows away from the black hole via jets of high-energy particles. Courtesy of NASA/CXC/A. Hobart.*

## 6. Concluding Remarks

In 1987, a conference panel on the physical simulation and visual representation of natural phenomena [UBR*87] discussed the need for cooperation between computer graphics researchers and computational scientists working in the physical sciences. One year later, in his Steven Coons Award lecture [Gre88], Greenberg also highlighted the importance of the application of computer graphics to science, engineering and design.

After elaborating this report, our impression is that the collaborations between physical sciences and computer graphics researchers still leave much to be desired, specially with respect to the simulation and rendering of plasma phenomena. However, it became evident that a substantial progress can be attained in this area once stronger cooperations are established. Although we cannot offer a magical formula to change this scenario, we believe that the opening of more direct communication channels, through which common needs and complementary resources can be identifyed, may serve as a powerful catalyst for this process.

## Acknowledgements

The authors are grateful to the anonymous reviewers for their helpful suggestions, and to the following researchers and organizations for granting us permission to use their images and photographs: D.J. Price, S. Rosswog, NASA/CXC/SAO, NASA/GSFC/TRACE, M. Weiss, A. Hobart, J. Curtis, D. Malin, J. Myers, NASA/Goddard Space Flight Center/Scientific Visualization Studio, P. Ljung, R. Stein, A. Nordlund, B. Gudiksen, D.R. Nadeau and M. Magnor. The authors would also woul like to thank T.F. Chen for proofreading an early draft of this document. The work presented in this paper was supported by the Natural Sciences and

Engineering Research Council of Canada (NSERC grant 238337) and the Canada Foundation for Innovation (CFI grant 33418).

## References

[ABN02] ABEL T., BRYAN G., NORMAN M.: The formation of the first star in the universe. *Science 295*, 5552 (January 2002), 93–98. 20

[Aka94] AKASOFU S.: *The Amazing Northern Lights*. Alaska Geographic, Anchorage, Alaska, 1994. 4

[AML*04] ABBETT W., MIKIC Z., LINKER J., MCTIERNAN J., MAGARA T., FISHER G.: The photospheric boundary of Sun-to-Earth coupled models. *Journal of Atmospheric and Solar-Terrestrial Physics 66* (2004), 1257–1270. 11

[And01] ANDERSON U.: *Time-Domain Methods for the Maxwell Equations*. PhD thesis, Department of Numerical Analysis and Computer Science, Royal Institute of Technology, Sweden, February 2001. 9

[Ang69] ANGSTRÖM A.: Spectrum des nordlichts. *Ann. Phys. 137* (1869), 161. 4

[AR06] ARMITAGE P., REYNOLDS C.: The variability of accretion onto Schwarzschild black holes from turbulent magnetized discs. *Mon. Not. Roy. Astron. Soc. 341* (2006), 1041–1051. 13

[BB03] BELL I., BARANOSKI G.: More than RGB: moving toward spectral color reproduction. ACM SIGGRAPH Course Notes, San Diego, California, U.S.A., July 2003. Course 24. 2, 19

[BDG*03] BRODLIET K., DUCE D., GALLOP J., WALTON J., WOOD J.: Distributed and collaborative visualization. In *Eurographics - State of the Art Reports* (2003), pp. 139–166. 10

[BE94] BREKKE A., EGELAND A.: *The Northern Lights, Their Heritage and Science*. Gröndahl og Dreyers Forlag, AS, Oslo, 1994. 4, 7, 16

[Bit04] BITTENCOURT J.: *Fundamentals of Plasma Physics*, 3rd ed. Springer-Verlag, New York, U.S.A., 2004. 2, 3, 4, 5, 6

[BL91] BIRDSALL C., LANGDON A.: *Plasma Physics via Computer Simulation*. Institute of Physics Publishing, Bristol, U.K., 1991. 2, 9

[BOM06] BANERJEE A., OGALE A., MITRA K.: Experimental simulation of lightning optical emissions in clouds. *Journal of Physics D: Applied Physics 39* (2006), 575–583. 5

[Bow05] BOWMAN K.: *An Introduction to Programming with IDL: Interactive Data Language*. Academic Press, New York, 2005. 14, 15

[BR02] BARANOSKI G., ROKNE J.: Using a HPC system for the simulation of the trajectories of solar wind particles in the ionosphere. In *High Performance Computing Systems and Applications* (Norwell, Massachusetts, 2002), Dimopoulos N., Li K., (Eds.), Kluwer Academic Publishers, pp. 317–329. 19

[Bre97] BREKKE A.: *Physics of the Upper Polar Atmosphere*. John Wiley & Sons in association with Praxis Publishing, Chichester, U.K., 1997. 4

[BRS*00] BARANOSKI G., ROKNE J., SHIRLEY P., TRONDSEN T., BASTOS R.: Simulating the aurora borealis. In *8th Pacific Conference on Computer Graphics and Applications* (Los Alamitos, California, U.S.A., October 2000), IEEE Computer Society, pp. 2–14. 16

[BRS*03] BARANOSKI G., ROKNE J., SHIRLEY P., TRONDSEN T., BASTOS R.: Simulating the aurora. *The Journal of Visualization and Computer Animation 14*, 1 (February 2003), 43–59. 16

[Bry99] BRYANT D. A.: *Electron Acceleration in the Aurora and Beyond*. Institute of Physics Publishing, Bristol, UK, 1999. 4

[BS93] BOROVSKY J., SUSZCYNSKY D.: Optical measurements of the fine structure of auroral arcs. In *Auroral Plasma Dynamics* (Washington, D.C., 1993), Lysak R., (Ed.), American Geophysical Union, pp. 25–30. vol. 80 of Geophys. Monogr. Series. 16

[BSBD91] BOROVSKY J., SUSZCYNSKY D., BUCHWALD M., DEHAVEN H.: Measuring the thickness of auroral curtains. *Arctic 44*, 3 (1991), 231–238. 16

[Bur00] BURTNYK K.: Anatomy of an aurora. *Sky & Telescope 99*, 3 (March 2000), 35–40. 4

[BWRB05] BARANOSKI G., WAN J., ROKNE J., BELL I.: Simulating the dynamics of auroral phenomena. *ACM Transactions on Graphics 24*, 1 (January 2005), 37–59. 9, 16

[Cas96] CASTLEMAN K.: *Digital Image Processing*. Prentice-Hall, New York, 1996. 16

[Che84] CHEN F.: *Introduction to Plasma Physics and Controlled Fusion*, second ed. Plenun Press, New York, 1984. 2, 3, 4, 5, 9

[Cho06] CHO A.: Scheme for boiling nuclear matter gathers steam at accelerator lab. *Science 312*, 5771 (April 2006), 190–191. 3

[CJP02] CHEN Y., JONES S., PARKER S.: Gyrokinetic turbulence simulations with fully kinetic electrons. *IEEE Transactions on Plasma Science 30*, 1 (February 2002), 74–75. 1, 10

[Cla06] CLARK S.: The dark side of the sun. *Nature 441*, 7092 (May 2006), 402–404. 4

[CTOJ02] CEN R., TRIPP T., OSTRIKER J., JENKINS E.: Revealing the warm-hot intergalatic medium with O VI absorption. *The Astrophysical Journal 559* (September 2002), 5–8. 20

[CW00] CHAN T., WAN W.: Robust multigrid methods for elliptic linear systems. *J. Comput. Appl. Math. 123* (2000), 323–352. 16

[Das04] DAS A.: *Space Plasma Physics: An Introduction*. Narosa Publishing House, New Delhi, India, 2004. 2

[DCWP02] DEVLIN K., CHALMERS A., WILKIE A., PURGATHOFER W.: Tone reproduction and physically based spectral rendering. In *Eurographics - State of the Art Reports* (2002), pp. 101–123. 2, 19

[DH23] DEBYE P., HÜCKEL E.: On the debye length in strong electrolytes. *Physikal. Z. 24*, 9 (1923), 185–206. 3

[DLYM00] DICKMANN M., LJUNG P., YNNERMAN A., MCCLEMENTS K.: Large-scale numerical simulations of ion beam instabilities in unmagnetized astrophysical plasmas. *Physics of Plasmas 7*, 2 (December 2000), 5171–5181. 12

[DLYM02] DICKMANN M., LJUNG P., YNNERMAN A., MCCLEMENTS K.: Three-dimensional visualization of electron acceleration in a magnetized plasma. *IEEE Transactions on Plasma Science 30*, 1 (February 2002), 20–21. 12

[DR81] DRAZIN P., REID W.: *Hydrodynamic Stability*. Cambridge University Press, Cambridge, U.K., 1981. 9

[DW00] DICARLO J., WANDELL B.: Rendering high dynamic range images. In *SPIE Electronic Imaging* (January 2000), vol. 3965, pp. 392–401. 19

[DYN01] DOBASHI Y., YAMAMOTO T., NISHITA T.: Efficient rendering of lightning taking into account scattering effects due to clouds and atmospheric particles. In *9th Pacific Conference on Computer Graphics and Applications - Pacific Graphics 2001* (2001), pp. 390–399. 15

[Eas93] EASTWOOD J.: Computational plasma physics. In *Plasma Physics: An Introductory Course* (Cambridge. U.K., 1993), Dendy R., (Ed.), Cambridge University Press, pp. 167–187. 2, 9, 10

[Eat80] EATHER R.: *Majestic Lights*. American Geophysical Union, Washington, D.C., U.S.A., 1980. 4, 19

[EWCB04] ELKINGTON S., WILTBERGER M., CHAN A., BAKER D.: Physical models of the geospace radiation environment. *Journal of Atmospheric and Solar-Terrestrial Physics 66* (2004), 1371–1387. 11

[Fer03] FERWERDA J.: Three varieties of realism in computer graphics. In *Proceedings of SPIE Human Vision and Electronic Imaging* (June 2003), The International Society for Optical Engineering, pp. 290–297. 10

[Fey88] FEYNMAN R.: *QED: The Strange Theory of Light and Matter*. Princeton University Press, Princeton, New Jersey, U.S.A., 1988. 6

[FLS64a] FEYNMAN R., LEIGHTON R., SANDS M.: *The Feynman Lectures on Physics*, vol. I. Addison-Wesley Publishing Company, Reading, Massachusetts, U.S.A., 1964. 2, 8

[FLS64b] FEYNMAN R., LEIGHTON R., SANDS M.: *The Feynman Lectures on Physics*, vol. II. Addison-Wesley Publishing Company, Reading, Massachusetts, U.S.A., 1964. 3, 4, 5

[FLS64c] FEYNMAN R., LEIGHTON R., SANDS M.: *The Feynman Lectures on Physics*, vol. III. Addison-Wesley Publishing Company, Reading, Massachusetts, U.S.A., 1964. 6

[FZP03] FLORINSKI V., ZANK G., POGORELOV N.: Galactic cosmic ray transport in the global heliosphere. *Journal of Geophysical Research 108*, A6 (2003), 1–16. 11

[Gaí89] GAÍDUKOV N.: Motion of ball lightning in an airflow through a wide circular opening in a flat screen. *Soviet Physics Technical Physics 34*, 2 (February 1989), 181–184. 16

[Gaí91] GAÍDUKOV N.: Hydrodynamic model of the passage of ball lightning through a narrow slot in a flat screen. *Soviet Physics Technical Physics 36*, 11 (November 1991), 1223–1227. 16

[GAL*97] GREENBERG D., ARVO J., LAFORTUNE E., TORRANCE K., FERWERDA J., WALTER B., TRUMBORE B., SHIRLEY P., PATTANAIK S., FOO S.: A framework for realistic image synthesis. In *SIGGRAPH Proceedings, Annual Conference Series* (1997), pp. 477–494. 2, 19

[GB05] GURNETT D., BHATTACHARJEE A.: *Introduction to Plasma Physics with Space and Laboratory Applications*. Cambridge University Press, Cambridge, U.K., 2005. 2, 3

[Gla00] GLASSNER A.: Andrew Glassner's notebook: The digital ceraunoscope: Synthetic thunder and lightning, part 1. *IEEE Computer Graphics & Applications 20*, 2 (2000), 89–93. 15

[GLW*98] GOODRICH C., LYON J., WILTBERGER M., LOPEZ R., PAPADOPOULOS K.: An overview of the impact of the January 10-11, 1997 magnetic cloud on the magnetosphere via global MHD simulation. *Geophysical Research Letters 25*, 14 (July 1998), 2537–2540. 11

[GMNC01] GARCIA M., MCCLINTOCK J., NARAYAN R., CALLANAN P.: New evidence for black hole event horizon from Chandra. *The Astrophysical Journal 533* (May 2001), 47–50. 6

[GN02] GUDIKSEN B., NORDLUND A.: Bulk heating and slender magnetic loops in the solar corona. *The Astrophysical Journal 572* (June 2002), 113–116. 1, 15

[GPZ*04] GOMBOSI T., POWELL K., ZEEEUW D., CLAUER C., HANSEN K., MANCHESTER W., RIDLEY A., ROUSSSEV I., ABD Q.F. STOUT I. S., TOTH G.: Solution-adaptive magnetohydrodynamics for space plasmas: Sun-to-Earth simulations. *Computing in Science & Engineering* (March 2004), 14–35. 9, 11

[GR95] GOLDSTON R., RUTHERFORD P.: *Introduction to Plasma Physics*. Institute of Physics Publishing, Bristol, U.K., 1995. 2, 4, 5, 16

[Gre88] GREENBERG D.: 1987 Steven A. Coons Award Lecture. *Computer Graphics 22*, 1 (February 1988), 7–14. 20

[GSL*04] GOODRICH C., SUSSMAN A., LYON J., SHAY M., CASSAK P.: The CISM code coupling strategy. *Journal of Atmospheric and Solar-Terrestrial Physics 66* (2004), 1469–1479. 11

[Gud06] GUDIKSEN B.: Images of coronal loops. Personal communication, June 2006. Institute of Theoretical Astrophysics, University of Oslo, Norway. 15, 19

[Hal76] HALLINAN T.: Auroral spirals. 2. theory. *Journal of Geophysical Research 81*, 22 (August 1976), 3959–3965. 16

[Hal81] HALLINAN T.: The distribution of vorticity in auroral arcs. In *Physics of Auroral Arc Formation* (Washington, D.C., U.S.A., 1981), Akasofu S., Kan J., (Eds.), American Geophysicsl Union. 16

[Haw88] HAWKING S.: *A Brief History of Time: From The Big Bang to Black Holes*. Bantam Press, London, U.K., 1988. 20

[HE88] HOCKNEY R., EASTWOOD J.: *Computer Simulation Using Particles*. Institute of Physics, Bristol, 1988. 2, 9

[HG41] HENYEY L., GREENSTEIN J.: Diffuse radiation in the galaxy. *Astrophysics Journal 93* (1941), 70–83. 15

[HG05] HUMBIRD D., GRAVES D.: Molecular dynamics simulations of plasma-surface interactions: Importance of visualization tools. *IEEE Transactions on Plasma Science 33*, 2 (April 2005), 226–227. 19, 20

[Hin75] HINZE J.: *Turbulence*. McGraw-Hill, New York, 1975. 9

[HMD02] HUGHES P., MILLER M., DUNCAN G.: Three-dimensional hydrodynamic simulations of relativistic extragalactic jets. *The Astrophysical Journal 572* (2002), 713–728. 20

[Hoc66] HOCKNEY R.: Computer experiment of anomalus diffusion. *The Physics of Fluids 9*, 9 (September 1966), 1826–1835. 8

[Ich86] ICHIMARU S.: *Plasma Physics An Introduction to Statistical Physics of Charged Particles*. The Benjamin/Cummings Publishing Company, Inc., Menlo Park, California, U.S.A., 1986. 3, 4, 5

[Jon74] JONES A.: *Aurora*. D. Reidel Publishing Company, Dordrecht, Holland, 1974. 7, 8

[Jos06] JOSHI C.: Plasma accelerators. *Scientifc American* (February 2006), 41–47. 1, 5, 6, 12

[JPK01] JONES S., PARKER S., KIM C.: Low-cost high-performance scientific visualization. *Computing in Science & Engineering 3*, 4 (July 2001), 12–17. 10

[KD83] KATSOULEAS T., DAWSON J.: A plasma wave accelerator - surfatron I. *IEEE Transactions on Nuclear Science 30*, 4 (August 1983), 3241–3243. 6

[Kil06] KILLIAN T.: Cool vibes. *Nature 441*, 7091 (May 2006), 297–298. 4

[KL04] KIM T., LIN M.: Physically based animation and rendering of lightning. In *12th Pacific Conference on Computer Graphics and Applications - Pacific Graphics 2004* (Los Alamitos, California, U.S.A., 2004), IEEE Computer Society, pp. 267–275. 15

[Kru99] KRUSZEWSKI P.: A probabilistic technique for the synthetic imagery of lightning. *Computers & Graphics 23*, 2 (1999), 287–293. 15

[Las99] LASOTA J.: Unmasking black holes. *Scientific American* (May 1999), 40–47. 12, 13

[LDAY00] LJUNG P., DIECKMANN M., ANDERSSON N., YNNERMAN A.: Interactive visualization of particle-in-cell simulations. In *IEEE Visualization* (2000), pp. 469–472. 12

[LDY02] LJUNG P., DIECKMANN M., YNNERMAN A.: Interactive visualization of large scale time varying data sets. In *ACM SIGGRAPH Conference Abstracts and Applications* (2002), p. 204. 1, 12

[LH68] LEVY R., HOCKNEY R.: Computer experiments on low-density crossed-field electron beams. *The Physics of Fluids 11*, 4 (April 1968), 766–771. 12, 16

[Lju00] LJUNG P.: *Interactive Visualization of Particle In Cell Simulations*. Master's thesis, Department of Science and Technology, Linköping University, Sweden, 2000. 12

[LRP97] LARSON G., RUSHMEIER H., PIATKO C.: A visibility matching tone reproduction operator for high dynamic scenes. *IEEE Transactions on Visualization and Computer Graphics 3*, 4 (1997), 291–306. 2

[LSL*04] LUHMANN J., SOLOMON S., LINKER J., LYON J., MIKIC Z., ODSTRCIL D., WANG W., WILTBERGER M.: Coupled model simulation of a Sun-to-Earth space weather event. *Journal of Atmospheric and Solar-Terrestrial Physics 66* (2004), 1243–1256. 11

[Mal89] MALIN S.: *The Greenwich Guide to Stars, Galaxies and Nebulae*. Cambridge University Press, Cambridge. U.K., 1989. 7, 17

[Mal94] MALIN D.: *A View of the Universe*. Cambridge University Press, Cambridge, U.K., 1994. 7, 17

[MBDM97] MONTRYM J., BAUM D., DIGNAM D., MIGDAL C.: InfiniteReality: A real-time graphics system. *SIGGRAPH Proceedings, Annual Conference Series* (1997), 293–302. 12

[MDY*01] McClements K., Dieckmann M., Ynnerman A., Chapman S., Dendy R.: Surfatron and stochastic acceleration of electrons at supernova remnant shocks. *Physical Review Letters 87*, 25 (December 2001), 255002(1)–255002(4). 12

[MFF02] McKee G., Fenzi C., Fonck R.: Images of turbulence in a tokamak plasma. *IEEE Transactions on Plasma Science 30*, 1 (February 2002), 62–63. 10

[MHLH05] Magnor M., Hildebrand K., Lintu A., Hanson A.: Reflection nebula visualization. In *IEEE Visualization* (2005), pp. 255–262. 17

[MKHD04] Magnor M., Kindlmann G., Hansen C., Duric N.: Constrained inverse volume rendering for planeary nebulae. In *IEEE Visualization* (2004), pp. 83–90. 17

[MKHD05] Magnor M., Kindlmann G., Hansen C., Duric N.: Reconstruction and visualization of planetary nebulae. *IEEE Transactions on Visualization and Computer Graphics 11*, 5 (2005), 485–496. 17

[Mon05] Monaghan J.: Smoothed particle hydrodynamics. *Reports on Progress in Physics 68* (2005), 1703–1759. 9

[Nad00] Nadeau D.: Volume scene graphs. In *IEEE Symposium on Volume Visualization* (2000), pp. 49–57. 17

[Nat95] National Research Council: *Plasma Science From Fundamental Research to Technological Applications*. The National Academies Press, Washington, D.C., U.S.A., 1995. 1, 10

[Nat03] National Research Council: *The Sun to the Earth - and Beyond*. The National Academies Press, Washington, D.C., U.S.A., 2003. 1, 10, 11

[Nat04] National Research Council: *Plasma Physics of the Local Cosmos*. The National Academies Press, Washington, D.C., U.S.A., 2004. 11, 20

[NC01] Nevins W., Cohen B.: *Direct Numerical Simulation of Plasma Microturbulence*. Lawrence Livermore National Laboratory, U.S. Department of Energy, August 2001. UCRL-JC-144913. 1

[NGN*01] Nadeau D., Genetti J., Napear S., Pailthorpe B., Emmart C., Wesselak E., Davidson D.: Visualizing stars and emission nebulas. *Computer Graphics Forum 20*, 1 (March 2001), 27–33. 17

[NGS96] Nordlund A., Gaalsgard K., Stein R.: Visualizing astrophysical 3D MHD turbulence. In *Applied Parallel Computing (Lect. Notes in Comp. Sci., 1041)* (Berlin, 1996), Dongarra J., Madsen K.,, Wasniewski J., (Eds.), Springer-Verlag, pp. 450–461. 20

[Nor06] Normile D.: Waiting for ITER, fusion jocks look EAST. *Science 312*, 5776 (May 2006), 992–993. 5

[NPW84] Niemeyer L., Pietronero L., Wiesmann H.: Fractal dimension of dielectric breakdown. *Physical Review Letters 52*, 12 (1984), 1033–1037. 15

[NSB96] Nordlund A., Stein R., Brandenburg A.: Supercomputer windows into the solar convection zone. In *Windows on the Sun's Interior (Bull. of the Astronomical Soc. of India, 24)* (1996), Antia H., Chitre S., (Eds.), pp. 261–279. 14

[OB00] O'Dell C., Bally J.: Outflows, jets and shocks in the Orion nebula. *Revista Mexicana de Astronomia y Astrofisica (Serie De Conferencias) 9* (2000), 194–197. 17

[OC96] Ostlie D., Carrol B.: *An Introduction to Modern Stellar Astrophysics*. Addison-Wesley, Reading, Massachusets, U.S.A., 1996. 6, 8, 13, 14, 17

[Ode00] Odenwald S.: Solar storms: The silent menace. *Sky & Telescope 99*, 3 (March 2000), 41–56. 4

[OPL*04] Odstrcil D., Pizzo V., Linker J., Riley P., Lionello R., Mikic Z.: Initial coupling of coronal and heliospheric numerical magnetohydrodynamic codes. *Journal of Atmospheric and Solar-Terrestrial Physics 66* (2004), 1311–1320. 11

[PCS95] Parker S., Cummings J., Samtaney R.: Visualization of plasma turbulence. *IEEE Computer Graphics & Applications 15*, 2 (1995), 7–10. 10

[Pea97] Pearson T.: *PGPLOT Graphics Subroutine Library*. California Institute of Technology, U.S.A., 1997. Available online at: http://www.astro.caltech.edu/. 13

[PFK01] Partamies N., Freeman M., Kauristie K.: On the winding of auroral spirals: Interhemispheric observations and Hallinan's theory revisited. *Journal of Geophysical Research*, 106 (A12) (2001), 28913–28924. 16

[PM99] Paxton L., Meng C.: Auroral imaging and space-based optical remote sensing. *John Hopkins APL Technical Digest 20*, 4 (1999), 544–555. 4

[PR06] Price D., Rosswog S.: Producing ultrastrong magnetic fields in neutron star mergers. *Science 312*, 5774 (May 2006), 719–722. 12

[Pri06] Price D.: *Visualization of SPH data using SUPERSPHPLOT - v1.5.2*. School of Physics, University of Exeter, Exeter, U.K., May 2006. Available online at: http://www.astro.ex.ac.uk/people/dprice/supersphplot/. 12, 13

[RB67] Romick G., Belon A.: The spatial variation of auroral luminosity - I, determination of volume emission rate profiles. *Planetary Space Science 15* (1967), 1695–1716. 4, 18

[Ree83] Reeves W.: Particle systems - a technique for modeling a class of fuzzy objects. *Computer Graphics 17*, 3 (July 1983), 359–376. 16

[RW94] REED T., WYVILL B.: Visual simulation of lightning. In *SIGGRAPH Proceedings, Annual Conference Series* (July 1994), pp. 359–364. 15

[SDP04] SEMENOV V., DYADECHKIN S., PUNSLY B.: Simulation of jets driven by black hole rotation. *Science 305*, 5686 (August 2004), 978–980. 20

[SDRD99] SHAY M., DRAKE J., ROGERS B., DENTON R.: The scaling of collisionless, magnetic reconnection and large systems. *Geophysical Research Letters 26*, 14 (1999), 2163–2166. 11

[SF90] SILVESTER P., FERRARI R.: *Finite Elements for Electrical Engineers*, 2nd ed. Cambridge University Press, Cambridge, U.K., 1990. 9

[SFMC01] SOSORBARAM B., FUJIMOTO T., MURAOKA K., CHIBA N.: Visual simulation of lightning taking into account cloud growth. In *Computer Graphics International* (July 2001), IEEE Computer Society, pp. 89–95. 15

[SFW06] SPRINGEL V., FRENCK C., WHITE S.: The large-scale structure of the universe. *Nature 440*, 7088 (April 2006), 1137–1143. 20

[SGK*02] SCHARMER G., GUDIKSEN B., KISELMAN D., LOFDAHL M., VAN DER VOORF L.: Dark cores in sunspot penumbral filaments. *Nature 420* (November 2002), 151–153. 1

[Sho03] SHORE S.: *The Tapestry of Modern Astrophysics*. John Wiley & Sons, Hoboken, New Jersey, U.S.A., 2003. 6, 12, 14

[Sim04] SIMCOE R.: The cosmic web. *American Scientist 92*, 1 (2004), 30–40. 20

[SM81] SMITH H., MORGAN D.: The spectral characteristics of the visible radiation incident upon the surface of the Earth. In *Plants and the Daylight Spectrum* (London, U.K., January 1981), Smith H., (Ed.), Academic Press, pp. 3–20. 6

[SMSE00] SCHUSSMAN G., MA K., SCHISSEL D., EVANS T.: Visualizing DIII-D tokamak magnetic field lines. In *IEEE Visualization 2000* (2000), pp. 501–504. 10

[SN00] STEIN R., NORDLUND A.: Realistic solar convection simulations. *Solar Physics* (2000), 91–108. 14, 19

[Spr05] SPRINGEL V.: The cosmological simulation code GADGET-2. *Mon. Not. R. Astron. Soc. 364* (2005), 1105–1134. 19

[Ste00] STENHOFF M.: *Ball Lightning: An Unsolved Problem in Atmospheric Physics*. Kluwer Academic / Plenium Publishers, New York, N.Y., U.S.A., 2000. 15, 16

[Sup04] SUPLEE C.: A stormy star. *National Geographic* (July 2004), 2–33. 4, 14

[Taf00] TAFLOVE A.: *Computational Electrodynamics: The finite-difference time-domain method*, second ed. Artech House, Boston, M.A., U.S.A., 2000. 9

[Taj89] TAJIMA T.: *Computational Plasma Physics: With Applications to Fusion and Astrophysics*. Addison-Wesley, Redwood City, Ca, 1989. 17

[Tan02] TANG W.: Advanced computations in plasma physics. *Physics of Plasmas 9*, 5 (2002), 1856–1872. 9, 10, 19

[Tay01] TAYLOR K.: Auroras Earth's grand show of lights. *National Geographic* (November 2001), 48–63. 4, 10

[TBF00] THOMPSON D., BRAUN J., FORD R.: *OpenDX Paths to Visualization*. Visualization and Imagery Solutions, Inc., Montana, U.S.A., 2000. 10

[UBR*87] UPSON C., BARR A., REEVES B., WOLFF R., WOLFRAM S.: The physical simulation and visual representation of natural phenomena. *Computer Graphics 21*, 4 (1987), 355–356. 10, 11, 20

[Var04] VARSA P.: *A Physical Simulation of Ball Lightning for Computer Graphics*. Master's thesis, Department of Computer Science, The University of Calgary, Canada, March 2004. 15

[VK20] VEGARD L., KROGNESS Q.: The variation of light intensity along auroral ray-streamers. *Geofysiske Publikationer 1*, 1 (1920), 149–170. 16

[VK95] VOLAKIS J., KEMPEL L.: Electromagnetics: Computational methods and considerations. *IEEE Computational Science & Engineering 2*, 1 (1995), 42–57. 9

[VR06] VARSA P., ROKNE J.: Simulation of the ball lightning phenomenon. *Computers & Graphics* (2006). To appear. 15

[Wes91] WESTOVER L.: *Splatting: A Parallel, Feed-Forward Volume Rendering Algorithm*. PhD thesis, Department of Computer Science, University of North Carolina at Chapel Hill, North Carolina, U.S.A., November 1991. 16

[WNDS99] WOO M., NEIDER J., DAVIS T., SHREINER D.: *OpenGL Programming Guide*, third ed. Addison-Wesley, Reading, Massachusetts, USA, 1999. 12

[WO95] WEN Z., O'DELL C.: A three-dimensional model of the Orion nebula. *Astrophysical Journal 438*, 2 (January 1995), 784–793. 17

[YIIY01] YOSHIZAWA A., ITOH S., ITOH K., YOKOI N.: Turbulence theories and modelling of fluids and plasma. *Plasma Physics and Controlled Fusion 43* (2001), 1–144. 9

[Yos98] YOSHIZAWA A.: *Hydrodynamic and Magnetohydrodynamic Turbulent Flows: Modelling and Statistical Theory*. Kluver, Dordrecht, Holland, 1998. 9